doi.org/10.26434/chemrxiv.12910130.v1

Formation of the [Ge4O16Al48(OH)108(H2O)24]20+ Tetramer from Condensation of ε-GeAl12 Keggin Polycations

Mohammad Shohel, Jennifer Bjorklund, Jack Smith, Sara E. Mason, Tori Z. Forbes

Submitted date: 03/09/2020 • Posted date: 03/09/2020

Citation information: Shohel, Mohammad; Bjorklund, Jennifer; Smith, Jack; Mason, Sara E.; Forbes, Tori Z. (2020): Formation of the [Ge4O16Al48(OH)108(H2O)24]20+ Tetramer from Condensation of ε-GeAl12 Keggin Polycations. ChemRxiv. Preprint. https://doi.org/10.26434/chemrxiv.12910130.v1

Keggin-type polyaluminum cations belong to a unique class of polyoxometalates (POMs) with their large positive charge, hydroxo bridges, and divergent isomerization/oligomerization. Previously reported oligomerizations of the polyaluminum cations were driven solely by the δ-Keggin isomer, which created Al_{26}, Al_{30}, and Al_{32} dimeric species. We herein report the isolation of largest ever Keggin-type structure for this system through a unique mode of self-condensation among four ε-$GeAl_{12}^{8+}$ to form $[NaGe_4O_{16}Al_{48}(OH)_{108}(H_2O)_{24}]^{21+}(Ge_4Al_{48})$. Elemental analysis confirms the Ge^{4+} substitution, and dynamic light scattering experiments indicated that these larger species exist in the thermally aged solutions. DFT calculations have revealed that a single atom Ge substitution in tetrahedral site of ε-Al_{13}^{7+} is the key for the formation this cluster because it activates the deprotonation at certain octahedral sites to assist self-condensation in a specific mode.

File list (3)

SI_Ge4Al48_Shohel_ChemRxiv_09022020.docx (319.50 KiB)	view on ChemRxiv • download file
Ge4Al48_Shohel_ChemRxiv_09022020.pdf (772.28 KiB)	view on ChemRxiv • download file
Ge4Al48_Shohel_ChemRxiv_09022020.docx (2.67 MiB)	view on ChemRxiv • download file

Supplementary information

Formation of the $[Ge_4O_{16}Al_{48}(OH)_{108}(H_2O)_{24}]^{20+}$ tetramer from condensation of ε-$GeAl_{12}^{8+}$ Keggin polycations

Mohammad Shohel, Jennifer L. Bjorklund, Jack A. Smith, Sara E. Mason, Tori Z. Forbes*
Department of Chemistry, University of Iowa, Iowa City, IA-52242
*Corresponding authors: tori-forbes@uiowa.edu

Table of contents

1. Experimental Details

Synthesizing $Ge_4Al_{48}^{+20}$ and Crystallizing $Na[Ge_4O_{16}Al_{48}(OH)_{108}(H_2O)_{24}](2,6\text{-}NDS)_7Cl_7(H_2O)_{45}$

All chemicals, $AlCl_3 \cdot 6H_2O$ (Fisher Scientific), NaOH (Fisher Scientific), GeO_2 (BeanTown Chemicals), and 2,6-naphthalenedisulfonate disodium salt (97%, Sigma Aldrich), were used as received. Aqueous solutions in this study used ultrapure water (18.2 MΩ.cm, Easypure II) as the solvent. A solution contains ε-$GeAl_{12}$ was prepared by following general methodology of Lee et al., 2001 with some additional modification.[1] In a typical synthesis, 0.05 g of GeO_2 powder was added to 48 mL of a 0.25M NaOH solution and stirred until the solid was completely dissolved in the aqueous phase. This Ge^{4+} stock solution was heated to 85 °C and titrated with a 20 mL aliquot of a 0.25M $AlCl_3$ solution. After cooling to room temperature, 10 mL of this partially hydrolyzed Ge^{4+}/Al^{3+} stock solution was loaded into a 23 mL Teflon-lined Parr reaction vessel and aged in a gravimetric oven set at 90 °C for 7 days. This thermally aged solution was again allowed to slowly cool to room temperature and then a 4 mL aliquot was added to a glass scintillation vial. To create high-quality single crystals, a 2.6 mL of 2,6-napthalenedisulfonate solution (0.1M) was added to the vial, covered with perforated parafilm and allowed to slowly evaporate. After about 7 days, colorless, blocky crystals of **Ge_4Al_{48}** were formed alongside amorphous flocculants. The yields of the crystalline phase was determined by mechanical separation and was determined to be approximately 15% based upon Al. We evaluated other crystallizing agents (K_2SO_4, Na_2SeO_4 and 2,7-napthalenedisulfonate) over the course of this study, but only isolated the previously reported ε-$GeAl_{12}$ with Na_2SeO_4 (Space group= $I\bar{4}m2$, a= 13.002(4), b= 17.235(4), α= 90°).[1] However, the **Ge_4Al_{48}** compound could be reproducibly formed using the protocol described above.

Structural Characterization by Single Crystal X-ray Diffraction (SCXRD)

A small (80µm x 60µm x 20µm), but high-quality single crystal was separated from solvent using a needle with help of microscope and instantly coated in mineral oil on a MiTeGen micromount. The crystal was mounted in a Bruker D8 Quest single-crystal diffractometer equipped with a microfocus X-ray beam (Mo Kα; λ = 0.71073 Å) and a CMOS detector. Diffraction frames were collected at 100K (Oxford low-temperature cryosystem) with the Bruker APEX3 software package.[2] Peak intensities were corrected for Lorentz polarization, background effects, and absorption effects using the APEX3 software.[2] Initial structure solution was determined by intrinsic phasing and refined on the basis of F^2 for all unique data using the SHELXL 5 program.[3] The disordered solvents (H_2O) was modeled using SQUEEZE command in the Platon software during structure refinement[4]. Metal atoms and most of the oxygens in Ge_4Al_{48} cluster could be refined anisotropically. Hydrogen atoms associated with the 2,6-NDS and solvent molecules could not be assigned due to presence of disorder and partial occupancy.

Elemental Analysis by Inductively Coupled Plasma Mass Spectrometry (ICP-MS)

The concentration of Al, Ge and their molar ratio in Ge_4Al_{48} were determined in a Agilent 7900 ICP-MS system. A small amount (~5mg) Ge_4Al_{48} crystals were separated from the

amorphous flocculant by hand from three different crystallization replicates was dissolved separately in 2% nitric acid solution. A series of Al and Ge standard solutions were prepared in 2% nitric acid by diluting 1000 ppm ICP-MS standards bought from Fluka Analytical. Calibration curves constructed from standard solutions were used to determine the Ge:Al ratio of the dissolved crystalline materials and analysis was performed in triplicate.

Table S1: ICP-MS result of 2% nitric acid digested $Na[Ge_4O_{16}Al_{48}(OH)_{108}(H_2O)_{24}](2,6\text{-}NDS)_7Cl_7(H_2O)_{45}$ crystals.

Al concentration ppm	Al concentration (mol/L) x 10^4	Ge concentration ppm	Ge concentration (mol/L) x 10^5	Theoretical Ge based on Al (mol/L) x 10^5	Experimental $\frac{Al(mol)}{¿(mol)}$	Theoretical $\frac{Al(mol)}{¿(mol)}$
7.06± 4.23	2.62± 1.57	1.50± 0.92	2.06± 1.26	2.18	12.43± 0.45	12.0

Dynamic Light Scattering (DLS) measurement

The $GeAl_{12}^{8+}$ aqueous solution was aged at 90 °C for 7 days, cooled to room temperature and then the colloidal phase was allowed aggregate to the bottom of the vial. After 48 hours, the clear solution from top was filtered through a 0.25 µm membrane filter for dynamic light scattering measurement to determine hydrodynamic diameter using Zetasizer Nano ZS (Malvern instrument ltd, MA).

Computational Methodology

To better understand the differences in Keggin isomers, aqueous models of the ε- and δ-MAl_{12} (*M*= Al, Ga, Ge) Keggin nanoclusters were studied using density functional theory (DFT) as implemented in the DMol[3] quantum package developed by Delley.[5-6] Experimental crystal structures of ε-$GeAl_{12}^{8+}$ were obtained from Lee *et al.*;[1] ε-Al_{13}^{7+} from Parker *et al.*;[7] δ-Al_{13}^{7+} from Son *et al.*;[8] and $Ge_4Al_{48}^{20+}$ presented here. The experimental structures were used to create isolated molecular models, with hydrogen placement determined by bond valence to fulfill bonding requirements and stoichiometry. As previously used to study aluminum oxide nanomaterials,[9-12] aperiodic all-electron calculations were performed using the using the GGA-PBE[13] level of theory, using the double-numeric polarized (DNP) atom-centered basis set and a real-space global cutoff of 4.5 Å Optimization of all structures was done with an energy convergence criteria of 0.0003 eV and a residual force criteria of at least 0.005 eV/Å on all atoms. The Keggin models were embedded in the conductor-like screening model (COSMO) to simulate aqueous solvent effects.[14]

Previous computational studies have benchmarked the methods employed here. In computing cluster energetics, DMol[3] relative energies at the PBE/DNP/COSMO level were compared to those obtained using Gaussian09 PBE0/TZVP/PCM for Al_{30} Keggin-type clusters containing 2 symmetry-equivalent Cu cations. As reported in Abeysinghe et al. 2013, the relative energies of Cu_2-Al_{30} configurations differed between the two methods by 0.1 eV (or 4×10^{-4} eV/atom) for

clusters consisting of 238 atoms (2 Cu, 30 Al, 94 O, and 112 H)[15]. Additional testing compared the relative energies of $GaAl_{12}$ clusters, with varied positions of Ga, calculated at the PBE and B3LYP level (all other computational details consistent). The results showed maximum energy differences within 0.1 eV between different and optimized tetrahedral Ga-O bond lengths within numerical precision of one another. As such, the GGA-PBE functional is an appropriate functional choice for studying these oxyhydroxide clusters in terms of balancing computational cost and accuracy. Testing was also done to compare how basis set quality influences relative energies of two Al_{13} isomers, comparing the polarized double (DNP) and triple-numeric (TNP) basis sets.[16] The energy difference between the ε- and δ-isomers was found to be 0.072 eV for DNP and 0.086 for TNP; as the computed differences in relative energy are of a similar magnitude, it can be concluded that DNP is a suitable choice in basis set.

Calculations of the isolated ε- and δ-MAl_{12} nanoclusters were used to compare relative stability of the isomers, where M= Al or Ge. Interactions of ε-Al_{13} and ε-$GeAl_{12}$ with SO_4^{2-} were sampled, taking note of instances where the anion interaction resulted in cluster deprotonation. The change in Mulliken charge population (Δq_M) provides a metric for comparing charge transfer or the degree of electron sharing between the Keggin and the anion, given in units of fundamental electron charge (e). Values of Δq_M are calculated by summing the partial atomic charges of the sulfate anion and determining the change from the initial formal charge of -2 e. Previous studies have shown that interactions resulting in anion Δq_M values greater than 0.50 e undergo deprotonation.[9-10] Calculated Δq_M values for different sites of ε and δ isomers are listed in Table S1 and Table S2 respectively.

Table S2: ε-isomer Δq_M values for SO_4^{2-} interactions, in units of fundamental electron charge (e). Deprotonation interactions are highlighted in boldface.

Keggin	Site 1	Site 2
ε-$GeAl_{12}$	**0.67**	0.39
ε-Al_{13}	0.41	0.34

Table S3: δ-isomer Δq_M values for SO_4^{2-} interactions, in units of fundamental electron charge (e). Deprotonation interactions are highlighted in boldface.

Keggin	Site 1	Site 2	Site 3
δ-$GeAl_{12}$	**0.66**	**0.65**	**0.59**
δ-Al_{13}	0.40	**0.61**	0.40

2. Crystallographic Information

Table S4: Crystal data and structure refinement for $Na[Ge_4O_{16}Al_{48}(OH)_{108}(H_2O)_{24}](2,6\text{-}NDS)_7Cl_7(H_2O)_{45}$

Empirical formula	$C_{145}HAl_{96}Cl_{14.25}Ge_8Na_2O_{471}S_{29.25}$

Formula weight	6968.575
Temperature/K	100(2)
Crystal system	monoclinic
Space group	$P2_1/c$
a/Å	36.786(4)
b/Å	35.861(3)
c/Å	48.892(5)
α/°	90
β/°	92.744(2)
γ/°	90
Volume/$Å^3$	64423(11)
Z	2
$\rho_{calc}g/cm^3$	1.370
μ/mm^{-1}	0.756
F(000)	27497.0
Crystal size/mm^3	0.100 × 0.080 × 0.080
Radiation	MoKα (λ = 0.71073)
2Θ range for data collection/°	4.22 to 38.422
Index ranges	$-34 \le h \le 34$, $-33 \le k \le 33$, $-45 \le l \le 45$
Reflections collected	741942
Independent reflections	53480 [R_{int} = 0.1668, R_{sigma} = 0.0571]
Data/restraints/parameters	53480/0/5389
Goodness-of-fit on F^2	0.939
Final R indexes [I>=2σ (I)]	R_1 = 0.1047, wR_2 = 0.2644
Final R indexes [all data]	R_1 = 0.1454, wR_2 = 0.3065
Largest diff. peak/hole / e $Å^{-3}$	2.87/-1.45

Table S5: Selected bond distances for $Ge_4Al_{48}^{20+}$

Atom	Atom	Length/Å		Atom	Atom	Length/Å
Ge01	O28	1.766(10)		Al48	O130	1.982(10)
Ge01	O11	1.773(10)		Ge05	O276	1.764(11)
Ge01	O126	1.775(10)		Ge05	O271	1.777(10)
Ge01	O27	1.785(10)		Ge05	O277	1.786(10)
Ge02	O119	1.775(11)		Ge05	O267	1.806(10)
Ge02	O116	1.779(10)		Ge06	O247	1.774(10)
Ge02	O140	1.787(10)		Ge06	O238	1.778(11)
Ge02	O118	1.791(10)		Ge06	O246	1.779(11)
Ge03	O57	1.782(10)		Ge06	O236	1.792(11)
Ge03	O58	1.789(10)		Ge07	O164	1.760(11)
Ge03	O54	1.790(11)		Ge07	O169	1.760(11)

Ge03	O46	1.798(10)		Ge07	O293	1.778(10)
Ge04	O87	1.772(9)		Ge07	O157	1.799(11)
Ge04	O90	1.783(9)		Ge08	O204	1.762(12)
Ge04	O89	1.785(10)		Ge08	O206	1.779(11)
Ge04	O99	1.798(10)		Ge08	O203	1.781(12)
Al01	O129	1.844(11)		Ge08	O195	1.785(11)
Al01	O128	1.855(11)		Al49	O153	1.817(13)
Al01	O06	1.856(11)		Al49	O162	1.838(13)
Al01	O03	1.856(11)		Al49	O163	1.838(15)
Al01	O02	1.926(11)		Al49	O156	1.869(15)
Al01	O126	2.057(10)		Al49	O165	1.918(13)
Al01	Al04	2.892(7)		Al49	O157	2.087(12)
Al01	Al02	2.978(6)		Al49	Al50	2.855(10)
Al01	Al03	2.990(7)		Al49	Al87	2.988(9)
Al02	O125	1.849(10)		Al50	O172	1.844(12)
Al02	O127	1.851(10)		Al50	O162	1.850(14)
Al02	O03	1.853(11)		Al50	O163	1.851(13)
Al02	O05	1.861(11)		Al50	O171	1.862(14)
Al02	O01	1.953(10)		Al50	O170	1.954(13)
Al02	O126	2.085(10)		Al50	O169	2.020(12)
Al02	Al48	2.868(7)		Al50	Al88	2.963(8)
Al02	Al03	2.990(7)		Al51	O279	1.840(12)
Al03	O05	1.830(11)		Al51	O264	1.846(11)
Al03	O07	1.836(11)		Al51	O290	1.851(11)
Al03	O06	1.842(11)		Al51	O266	1.853(11)
Al03	O08	1.866(11)		Al51	O280	1.922(12)
Al03	O04	1.918(11)		Al51	O267	2.108(11)
Al03	O126	2.151(10)		Al51	Al70	2.867(7)
Al03	Al05	2.887(7)		Al51	Al53	2.998(7)
Al04	O25	1.841(11)		Al51	Al52	2.999(7)
Al04	O129	1.854(11)		Al52	O262	1.839(12)
Al04	O26	1.860(11)		Al52	O264	1.844(11)
Al04	O128	1.873(11)		Al52	O261	1.854(11)
Al04	O23	1.950(11)		Al52	O265	1.880(11)
Al04	O27	2.007(10)		Al52	O263	1.925(11)
Al05	O12	1.849(11)		Al52	O267	2.077(10)
Al05	O13	1.852(11)		Al52	Al58	2.887(7)
Al05	O08	1.857(11)		Al52	Al53	2.998(7)
Al05	O07	1.863(11)		Al53	O279	1.830(12)
Al05	O09	1.944(11)		Al53	O282	1.842(11)

Al05	O11	1.990(11)		Al53	O265	1.857(11)
Al05	Al09	2.989(7)		Al53	O283	1.860(11)
Al06	O24	1.837(11)		Al53	O281	1.912(11)
Al06	O25	1.848(11)		Al53	O267	2.076(10)
Al06	O30	1.849(11)		Al53	Al54	2.861(7)
Al06	O22	1.853(11)		Al54	O283	1.845(11)
Al06	O21	1.857(10)		Al54	O285	1.851(11)
Al06	O27	2.185(10)		Al54	O286	1.854(11)
Al06	Al08	2.864(7)		Al54	O282	1.877(11)
Al07	O22	1.848(11)		Al54	O284	1.910(11)
Al07	O26	1.853(11)		Al54	O277	2.033(11)
Al07	O18	1.853(10)		Al54	Al92	2.983(7)
Al07	O15	1.871(11)		Al55	O182	1.850(11)
Al07	O19	1.876(11)		Al55	O274	1.856(11)
Al07	O27	2.180(10)		Al55	O270	1.859(11)
Al07	Al09	2.871(7)		Al55	O289	1.860(11)
Al08	O21	1.857(10)		Al55	O273	1.880(11)
Al08	O20	1.859(11)		Al55	O276	2.152(11)
Al08	O146	1.860(11)		Al55	Al66	2.877(7)
Al08	O24	1.866(11)		Al55	Al70	2.969(7)
Al08	O29	1.868(11)		Al56	O274	1.840(11)
Al08	O28	2.151(10)		Al56	O219	1.851(11)
Al08	Al48	2.959(7)		Al56	O259	1.858(11)
Al09	O18	1.852(11)		Al56	O288	1.860(11)
Al09	O13	1.861(11)		Al56	O291	1.884(11)
Al09	O34	1.864(11)		Al56	O276	2.258(11)
Al09	O15	1.876(11)		Al56	Al62	2.864(7)
Al09	O32	1.883(11)		Al57	O248	1.846(12)
Al09	O11	2.149(11)		Al57	O249	1.850(11)
Al10	O17	1.840(11)		Al57	O240	1.855(12)
Al10	O10	1.843(11)		Al57	O243	1.877(12)
Al10	O14	1.847(11)		Al57	O244	1.972(11)
Al10	O31	1.849(11)		Al57	O247	2.013(11)
Al10	O20	1.854(11)		Al57	Al78	2.885(8)
Al10	O28	2.275(10)		Al57	Al64	2.988(7)
Al10	Al11	2.861(7)		Al58	O268	1.839(11)
Al11	O12	1.845(11)		Al58	O269	1.847(11)
Al11	O14	1.847(11)		Al58	O261	1.859(11)
Al11	O16	1.848(11)		Al58	O262	1.874(11)
Al11	O31	1.848(11)		Al58	O260	1.950(11)

Al11	O34	1.862(11)		Al58	O271	2.038(10)
Al11	O11	2.291(11)		Al59	O251	1.845(11)
Al12	O30	1.847(11)		Al59	O248	1.849(11)
Al12	O70	1.848(11)		Al59	O253	1.854(11)
Al12	O53	1.857(11)		Al59	O255	1.862(11)
Al12	O67	1.875(11)		Al59	O176	1.868(12)
Al12	O59	1.878(11)		Al59	O247	2.197(11)
Al12	O58	2.182(11)		Al59	Al95	2.865(7)
Al12	Al13	2.870(7)		Al60	O176	1.843(12)
Al13	O29	1.852(11)		Al60	O161	1.852(11)
Al13	O67	1.857(11)		Al60	O179	1.854(11)
Al13	O51	1.860(12)		Al60	O177	1.861(11)
Al13	O64	1.863(11)		Al60	O168	1.874(12)
Al13	O53	1.878(11)		Al60	O164	2.246(11)
Al13	O54	2.115(12)		Al60	Al96	2.882(7)
Al13	Al30	2.986(7)		Al61	O201	1.847(12)
Al14	O108	1.836(11)		Al61	O211	1.851(12)
Al14	O122	1.846(12)		Al61	O217	1.859(12)
Al14	O109	1.853(11)		Al61	O220	1.864(12)
Al14	O121	1.861(11)		Al61	O221	1.881(12)
Al14	O17	1.874(11)		Al61	O203	2.173(11)
Al14	O118	2.257(12)		Al61	Al63	2.859(8)
Al14	Al15	2.862(7)		Al61	Al79	2.997(7)
Al15	O108	1.844(11)		Al62	O287	1.847(11)
Al15	O16	1.856(11)		Al62	O259	1.856(11)
Al15	O122	1.858(11)		Al62	O285	1.860(11)
Al15	O33	1.860(12)		Al62	O288	1.863(12)
Al15	O107	1.864(11)		Al62	O221	1.870(11)
Al15	O119	2.245(11)		Al62	O277	2.172(11)
Al16	O91	1.849(11)		Al63	O215	1.848(12)
Al16	O124	1.854(11)		Al63	O219	1.863(12)
Al16	O32	1.860(11)		Al63	O213	1.865(12)
Al16	O77	1.863(10)		Al63	O211	1.866(12)
Al16	O76	1.864(10)		Al63	O217	1.868(12)
Al16	O89	2.207(10)		Al63	O204	2.213(11)
Al16	Al28	2.885(6)		Al64	O253	1.846(11)
Al16	Al25	2.996(6)		Al64	O252	1.862(12)
Al17	O121	1.844(12)		Al64	O149	1.862(10)
Al17	O117	1.871(12)		Al64	O257	1.871(11)
Al17	O138	1.872(13)		Al64	O249	1.872(11)

Al17	O141	1.875(12)		Al64	O247	2.180(11)
Al17	O139	1.950(12)		Al64	Al94	2.872(7)
Al17	O118	1.970(11)		Al65	O257	1.840(11)
Al17	Al21	2.895(8)		Al65	O269	1.852(10)
Al17	Al18	2.986(7)		Al65	O272	1.856(10)
Al18	O111	1.853(11)		Al65	O275	1.857(10)
Al18	O117	1.863(11)		Al65	O278	1.858(11)
Al18	O115	1.863(12)		Al65	O271	2.200(10)
Al18	O109	1.871(11)		Al65	Al92	2.865(7)
Al18	O63	1.881(12)		Al66	O268	1.846(11)
Al18	O118	2.123(11)		Al66	O181	1.855(11)
Al18	Al24	2.865(7)		Al66	O270	1.869(11)
Al19	O81	1.850(10)		Al66	O273	1.870(11)
Al19	O120	1.860(11)		Al66	O272	1.872(11)
Al19	O145	1.864(11)		Al66	O271	2.137(10)
Al19	O107	1.865(11)		Al67	O159	1.827(11)
Al19	O110	1.878(11)		Al67	O161	1.853(11)
Al19	O119	2.090(11)		Al67	O154	1.862(12)
Al19	Al47	2.875(7)		Al67	O155	1.866(12)
Al19	Al20	2.976(7)		Al67	O152	1.963(11)
Al20	O33	1.836(12)		Al67	O164	2.027(11)
Al20	O120	1.837(12)		Al67	Al82	2.888(7)
Al20	O137	1.854(12)		Al67	Al93	2.992(7)
Al20	O148	1.872(12)		Al68	O216	1.843(12)
Al20	O136	1.936(13)		Al68	O205	1.849(14)
Al20	O119	2.017(12)		Al68	O214	1.849(13)
Al20	Al46	2.870(9)		Al68	O212	1.863(13)
Al21	O147	1.849(15)		Al68	O207	1.874(13)
Al21	O134	1.866(17)		Al68	O206	2.235(13)
Al21	O138	1.874(13)		Al68	Al69	2.852(8)
Al21	O141	1.893(13)		Al69	O220	1.849(12)
Al21	O133	1.933(15)		Al69	O218	1.857(13)
Al21	O140	2.098(11)		Al69	O216	1.859(13)
Al21	Al46	2.970(9)		Al69	O205	1.861(12)
Al21	Al22	2.974(9)		Al69	O202	1.863(13)
Al22	O135	1.825(16)		Al69	O203	2.196(13)
Al22	O147	1.826(15)		Al70	O289	1.845(11)
Al22	O143	1.873(14)		Al70	O290	1.850(12)
Al22	O142	1.886(13)		Al70	O291	1.850(11)
Al22	O131	1.939(16)		Al70	O266	1.856(11)

Al22	O140	2.111(12)		Al70	O292	1.947(11)
Al22	Al23	2.880(9)		Al70	O276	2.000(11)
Al22	Al46	2.983(10)		Al71	O209	1.842(12)
Al23	O114	1.856(11)		Al71	O174	1.851(13)
Al23	O143	1.857(13)		Al71	O208	1.863(13)
Al23	O142	1.864(13)		Al71	O214	1.863(13)
Al23	O113	1.869(12)		Al71	O222	1.892(12)
Al23	O144	1.928(14)		Al71	O206	2.112(13)
Al23	O116	1.999(12)		Al71	Al74	2.858(8)
Al23	Al47	2.974(7)		Al71	Al86	2.976(8)
Al24	O112	1.844(11)		Al72	O235	1.835(13)
Al24	O65	1.852(12)		Al72	O242	1.844(13)
Al24	O115	1.854(11)		Al72	O250	1.851(12)
Al24	O113	1.854(12)		Al72	O245	1.864(12)
Al24	O111	1.874(11)		Al72	O241	1.945(14)
Al24	O116	2.193(11)		Al72	O246	2.020(12)
Al25	O88	1.825(11)		Al72	Al83	2.843(8)
Al25	O96	1.832(11)		Al72	Al94	2.977(7)
Al25	O91	1.835(11)		Al73	O189	1.834(14)
Al25	O94	1.877(10)		Al73	O190	1.849(15)
Al25	O95	1.948(11)		Al73	O197	1.879(14)
Al25	O89	2.035(11)		Al73	O198	1.884(13)
Al25	Al45	2.876(7)		Al73	O191	1.909(14)
Al25	Al26	2.994(7)		Al73	O195	2.074(14)
Al26	O88	1.850(10)		Al73	Al79	2.898(8)
Al26	O124	1.860(11)		Al73	Al76	2.965(10)
Al26	O79	1.864(11)		Al73	Al77	2.974(9)
Al26	O86	1.871(11)		Al74	O222	1.853(12)
Al26	O81	1.873(11)		Al74	O186	1.856(13)
Al26	O89	2.136(10)		Al74	O209	1.858(13)
Al26	Al27	2.864(7)		Al74	O215	1.866(11)
Al27	O86	1.839(11)		Al74	O210	1.874(13)
Al27	O73	1.851(11)		Al74	O204	2.147(12)
Al27	O84	1.857(11)		Al74	Al89	2.994(7)
Al27	O79	1.873(11)		Al75	O186	1.855(12)
Al27	O80	1.883(10)		Al75	O185	1.856(12)
Al27	O87	2.170(10)		Al75	O180	1.864(13)
Al28	O74	1.849(10)		Al75	O178	1.877(13)
Al28	O77	1.856(10)		Al75	O183	1.883(12)
Al28	O75	1.856(10)		Al75	O293	2.139(11)

Al28	O76	1.864(10)		Al75	Al88	2.864(8)
Al28	O19	1.866(11)		Al75	Al80	2.983(8)
Al28	O90	2.170(10)		Al76	O190	1.820(15)
Al28	Al40	2.997(6)		Al76	O223	1.840(14)
Al29	O55	1.844(11)		Al76	O187	1.842(15)
Al29	O64	1.846(11)		Al76	O196	1.867(13)
Al29	O63	1.856(11)		Al76	O188	1.944(15)
Al29	O66	1.861(12)		Al76	O195	2.106(14)
Al29	O52	1.861(11)		Al76	Al89	2.865(9)
Al29	O54	2.188(11)		Al76	Al77	2.973(10)
Al29	Al38	2.881(7)		Al77	O189	1.827(16)
Al30	O52	1.821(12)		Al77	O193	1.852(14)
Al30	O51	1.838(12)		Al77	O187	1.857(16)
Al30	O44	1.849(12)		Al77	O194	1.868(15)
Al30	O43	1.854(12)		Al77	O294	1.930(15)
Al30	O39	1.943(12)		Al77	O195	2.093(13)
Al30	O54	2.057(11)		Al77	Al86	2.865(9)
Al30	Al31	2.871(8)		Al78	O233	1.840(13)
Al31	O41	1.825(13)		Al78	O243	1.849(12)
Al31	O44	1.844(13)		Al78	O226	1.853(13)
Al31	O40	1.848(13)		Al78	O240	1.863(13)
Al31	O43	1.854(13)		Al78	O234	1.912(12)
Al31	O38	1.914(13)		Al78	O236	2.087(12)
Al31	O46	2.122(11)		Al78	Al83	2.991(8)
Al31	Al32	2.987(8)		Al78	Al85	2.994(8)
Al31	Al34	2.988(8)		Al79	O201	1.851(12)
Al32	O49	1.844(12)		Al79	O198	1.856(13)
Al32	O45	1.855(12)		Al79	O202	1.865(13)
Al32	O42	1.855(12)		Al79	O197	1.866(13)
Al32	O40	1.858(12)		Al79	O199	1.935(14)
Al32	O37	1.920(12)		Al79	O203	1.997(13)
Al32	O46	2.097(12)		Al80	O166	1.837(12)
Al32	Al33	2.869(7)		Al80	O180	1.847(13)
Al32	Al34	2.981(8)		Al80	O158	1.848(12)
Al33	O62	1.843(11)		Al80	O160	1.874(13)
Al33	O59	1.853(11)		Al80	O295	1.936(13)
Al33	O49	1.857(11)		Al80	O293	2.037(12)
Al33	O45	1.858(12)		Al80	Al87	2.859(8)
Al33	O47	1.974(12)		Al80	Al91	2.988(7)
Al33	O58	2.008(11)		Al81	O231	1.840(15)

Al34	O48	1.836(13)		Al81	O230	1.850(13)
Al34	O50	1.853(12)		Al81	O229	1.858(14)
Al34	O42	1.855(12)		Al81	O228	1.864(13)
Al34	O41	1.858(13)		Al81	O224	1.950(13)
Al34	O35	1.930(13)		Al81	O238	2.006(11)
Al34	O46	2.040(12)		Al81	Al85	2.874(9)
Al34	Al36	2.869(8)		Al81	Al95	2.994(8)
Al35	O61	1.851(11)		Al82	O151	1.836(14)
Al35	O70	1.868(11)		Al82	O154	1.850(12)
Al35	O72	1.869(11)		Al82	O155	1.856(13)
Al35	O62	1.879(11)		Al82	O153	1.866(13)
Al35	O69	1.887(11)		Al82	O150	1.927(13)
Al35	O58	2.143(11)		Al82	O157	2.093(12)
Al35	Al37	2.856(7)		Al82	Al87	2.995(8)
Al36	O60	1.843(12)		Al83	O242	1.827(14)
Al36	O50	1.849(12)		Al83	O235	1.832(12)
Al36	O56	1.861(12)		Al83	O227	1.844(14)
Al36	O48	1.867(12)		Al83	O233	1.854(12)
Al36	O36	1.939(12)		Al83	O232	1.897(14)
Al36	O57	1.992(11)		Al83	O236	2.121(14)
Al36	Al37	2.977(7)		Al84	O212	1.854(12)
Al37	O61	1.858(11)		Al84	O230	1.857(12)
Al37	O68	1.859(11)		Al84	O237	1.864(14)
Al37	O69	1.866(11)		Al84	O256	1.865(11)
Al37	O71	1.873(11)		Al84	O239	1.868(13)
Al37	O60	1.873(11)		Al84	O238	2.204(12)
Al37	O57	2.125(11)		Al84	Al90	2.861(8)
Al38	O56	1.838(12)		Al85	O226	1.840(13)
Al38	O68	1.850(11)		Al85	O227	1.855(15)
Al38	O55	1.854(12)		Al85	O228	1.859(15)
Al38	O65	1.869(12)		Al85	O229	1.863(13)
Al38	O66	1.877(11)		Al85	O225	1.916(13)
Al38	O57	2.255(11)		Al85	O236	2.063(12)
Al39	O83	1.838(11)		Al86	O194	1.842(15)
Al39	O82	1.849(10)		Al86	O208	1.857(15)
Al39	O72	1.855(11)		Al86	O193	1.867(14)
Al39	O74	1.857(10)		Al86	O207	1.875(14)
Al39	O78	1.876(10)		Al86	O192	1.946(13)
Al39	O90	2.213(10)		Al86	O206	2.013(12)
Al39	Al41	2.868(7)		Al87	O160	1.844(12)

Al40	O82	1.854(10)		Al87	O158	1.855(13)
Al40	O75	1.854(10)		Al87	O156	1.864(15)
Al40	O100	1.867(11)		Al87	O151	1.865(13)
Al40	O93	1.878(11)		Al87	O296[1]	1.904(14)
Al40	O92	1.963(11)		Al87	O157	2.068(13)
Al40	O90	2.010(10)		Al88	O172	1.856(12)
Al40	Al42	2.890(6)		Al88	O183	1.860(13)
Al41	O85	1.833(11)		Al88	O178	1.863(12)
Al41	O83	1.848(11)		Al88	O174	1.864(12)
Al41	O71	1.858(11)		Al88	O173	1.880(12)
Al41	O80	1.872(11)		Al88	O169	2.113(12)
Al41	O78	1.890(10)		Al89	O213	1.850(12)
Al41	O87	2.189(10)		Al89	O210	1.855(13)
Al42	O100	1.840(11)		Al89	O223	1.857(13)
Al42	O103	1.843(11)		Al89	O196	1.858(14)
Al42	O93	1.847(11)		Al89	O200	1.945(14)
Al42	O102	1.850(10)		Al89	O204	2.013(12)
Al42	O101	1.912(11)		Al90	O256	1.841(13)
Al42	O99	2.095(10)		Al90	O245	1.847(13)
Al42	Al44	2.983(6)		Al90	O254	1.853(12)
Al42	Al45	2.987(6)		Al90	O218	1.856(12)
Al43	O85	1.840(11)		Al90	O237	1.861(13)
Al43	O98	1.848(11)		Al90	O246	2.196(11)
Al43	O97	1.850(11)		Al91	O167	1.837(11)
Al43	O84	1.857(11)		Al91	O166	1.839(12)
Al43	O123	1.913(11)		Al91	O185	1.859(12)
Al43	O87	2.032(10)		Al91	O182	1.867(11)
Al43	Al44	2.867(7)		Al91	O184	1.877(11)
Al44	O98	1.831(11)		Al91	O293	2.159(11)
Al44	O103	1.831(10)		Al91	Al93	2.869(7)
Al44	O104	1.855(11)		Al92	O258	1.845(11)
Al44	O97	1.868(10)		Al92	O286	1.849(11)
Al44	O105	1.926(11)		Al92	O275	1.850(11)
Al44	O99	2.053(10)		Al92	O287	1.855(11)
Al44	Al45	2.998(7)		Al92	O278	1.861(11)
Al45	O102	1.843(10)		Al92	O277	2.148(11)
Al45	O104	1.844(11)		Al93	O167	1.839(11)
Al45	O96	1.849(11)		Al93	O159	1.857(11)
Al45	O94	1.873(11)		Al93	O179	1.865(11)
Al45	O106	1.954(11)		Al93	O181	1.872(11)

Al45	O99	2.108(10)		Al93	O184	1.879(11)
Al46	O135	1.822(16)		Al93	O164	2.168(11)
Al46	O134	1.836(16)		Al94	O250	1.848(12)
Al46	O148	1.853(13)		Al94	O149	1.851(12)
Al46	O137	1.892(14)		Al94	O258	1.860(12)
Al46	O132	1.935(16)		Al94	O252	1.873(11)
Al46	O140	2.108(12)		Al94	O254	1.875(11)
Al47	O73	1.853(11)		Al94	O246	2.133(11)
Al47	O114	1.863(11)		Al95	O251	1.847(12)
Al47	O112	1.867(11)		Al95	O239	1.852(12)
Al47	O110	1.869(11)		Al95	O231	1.853(12)
Al47	O145	1.869(11)		Al95	O255	1.865(12)
Al47	O116	2.141(11)		Al95	O175	1.877(13)
Al48	O146	1.842(11)		Al95	O238	2.174(13)
Al48	O125	1.854(11)		Al96	O171	1.825(12)
Al48	O10	1.855(11)		Al96	O175	1.838(13)
Al48	O127	1.893(11)		Al96	O173	1.848(12)
Al48	O28	1.966(10)		Al96	O168	1.853(12)
				Al96	O177	1.875(11)
				Al96	O169	2.270(12)

3. Additional figures

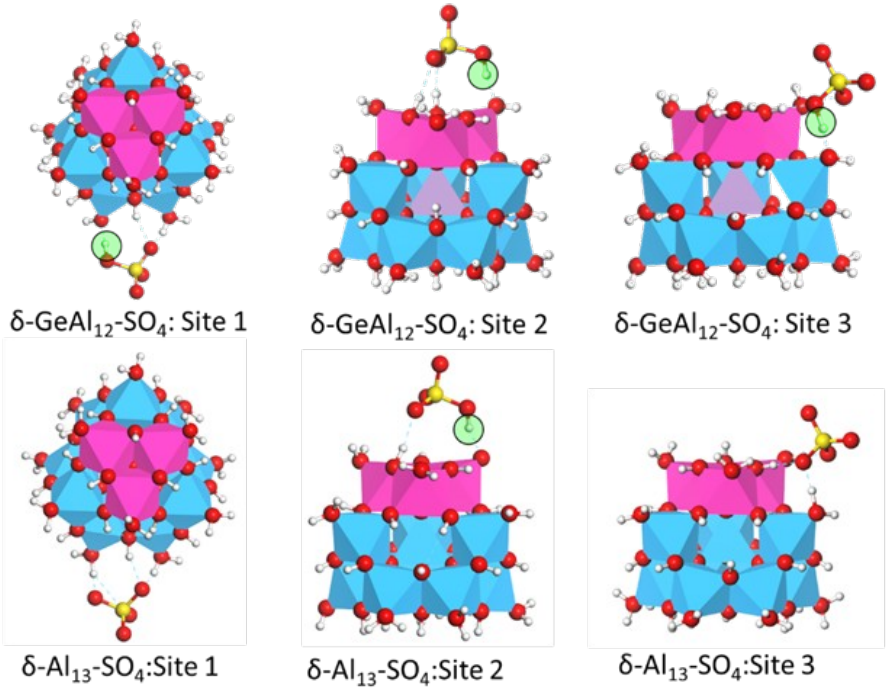

Figure S1. Different surface sites of δ- $GeAl_{12}$ and δ- Al_{13} interacting with SO_4^{2-} ion. The abstracted proton is highlighted with a green circle. Blue and purple polyhedra are used to represent Al and Ge atoms, respectively. Red, yellow and white balls are used to represent O, S, and H atoms, respectively.

References

1. Lee, A. P.; Phillips, B. L.; Olmstead, M. M.; Casey, W. H., Synthesis and Characterization of the GeO4Al12(OH)24(OH2)128+ Polyoxocation. *Inorganic Chemistry* **2001,** *40* (17), 4485-4487.
2. Bruker-AXS *APEX2*, 2014.11-0; Bruker AXS: Madison, Wisconsin, USA, 2014.
3. Sheldrick, G. M., Crystal structure refinement with SHELXL. *Acta Crystallographica Section C Structural Chemistry* **2015,** *71* (1), 3-8.
4. Spek, A., Single-crystal structure validation with the program PLATON. *Journal of Applied Crystallography* **2003,** *36* (1), 7-13.
5. Delley, B., An All-Electron Numerical-Method for Solving the Local Density Functional for Polyatomic-Molecules. *J Chem Phys* **1990,** *92* (1), 508-517.
6. Delley, B., From molecules to solids with the DMol(3) approach. *J Chem Phys* **2000,** *113* (18), 7756-7764.
7. Parker, W. O. N.; Millini, R.; Kiricsi, I., Metal Substitution in Keggin-Type Tridecameric Aluminum−Oxo−Hydroxy Clusters. *Inorganic Chemistry* **1997,** *36* (4), 571-575.

8. Son, J. H.; Kwon, Y.-U.; Han, O. H., New Ionic Crystals of Oppositely Charged Cluster Ions and Their Characterization. *Inorganic Chemistry* **2003,** *42* (13), 4153-4159.
9. Bennett, J. W.; Bjorklund, J. L.; Forbes, T. Z.; Mason, S. E., Systematic Study of Aluminum Nanoclusters and Anion Adsorbates. *Inorganic Chemistry* **2017,** *56* (21), 13014-13028.
10. Bjorklund, J. L.; Bennett, J. W.; Forbes, T. Z.; Mason, S. E., Modeling of MAl12 Keggin Heteroatom Reactivity by Anion Adsorption. *Crystal Growth & Design* **2019,** *19* (5), 2820-2829.
11. Abeysinghe, S.; Corum, K. W.; Neff, D. L.; Mason, S. E.; Forbes, T. Z., Contaminant Adsorption on Nanoscale Particles: Structural and Theoretical Characterization of Cu2+ Bonding on the Surface of Keggin-Type Polyaluminum (Al-30) Molecular Species. *Langmuir* **2013,** *29* (46), 14124-14134.
12. Corum, K. W.; Mason, S. E., Establishing trends in ion adsorption on the aqueous aluminium hydroxide nanoparticle Al-30. *Mol Simulat* **2015,** *41* (1-3), 146-155.
13. Perdew, J. P.; Burke, K.; Ernzerhof, M., Generalized gradient approximation made simple. *Phys Rev Lett* **1996,** *77* (18), 3865-3868.
14. Klamt, A.; Schuurmann, G., Cosmo - a New Approach to Dielectric Screening in Solvents with Explicit Expressions for the Screening Energy and Its Gradient. *Journal of the Chemical Society-Perkin Transactions 2* **1993,** (5), 799-805.
15. Abeysinghe, S.; Corum, K. W.; Neff, D. L.; Mason, S. E.; Forbes, T. Z., Contaminant Adsorption on Nanoscale Particles: Structural and Theoretical Characterization of Cu2+ Bonding on the Surface of Keggin-Type Polyaluminum (Al30) Molecular Species. *Langmuir* **2013,** *29* (46), 14124-14134.
16. Shohel, M.; Bjorklund, J. L.; Ovrom, E. A.; Mason, S. E.; Forbes, T. Z., Ga3+ Incorporation into Al13 Keggin Polyoxometalates and the Formation of δ-(GaAl12)7+ and (Ga2.5Al28.5)19+ Polycations. *Inorganic Chemistry* **2020,** *59* (15), 10461-10472.

Formation of the $[Ge_4O_{16}Al_{48}(OH)_{108}(H_2O)_{24}]^{20+}$ tetramer from condensation of ε-$GeAl_{12}$ Keggin polycations

Mohammad Shohel, Jennifer L. Bjorklund, Jack A. Smith, Sara E. Mason, Tori Z. Forbes*

Department of Chemistry, University of Iowa, Iowa City, IA-52242
*Corresponding author: tori-forbes@uiowa.edu

Supporting Information Placeholder

ABSTRACT: Keggin-type polyaluminum cations belong to a unique class of polyoxometalates (POMs) with their large positive charge, hydroxo bridges, and divergent isomerization/oligomerization. Previously reported oligomerizations of the polyaluminum cations were driven solely by the δ-Keggin isomer, which created Al_{26}, Al_{30}, and Al_{32} dimeric species. We herein report the isolation of largest ever Keggin-type structure for this system through a unique mode of self-condensation among four ε-$GeAl_{12}^{8+}$ to form $[NaGe_4O_{16}Al_{48}(OH)_{108}(H_2O)_{24}]^{21+}$(**$Ge_4Al_{48}$**). Elemental analysis confirms the Ge^{4+} substitution, and dynamic light scattering experiments indicated that these larger species exist in the thermally aged solutions. DFT calculations have revealed that a single atom Ge substitution in tetrahedral site of ε-Al_{13}^{7+} is the key for the formation this cluster because it activates the deprotonation at certain octahedral sites to assist self-condensation in a specific mode.

Since the discovery of Keggin-type polyoxometalates (POMs) in 1933,[1] chemists and material scientists have been fascinated by their unique structural features and applications in energy, medicine, and water purification. The Keggin topology was first identified as a phosphotungstate and contains a central tetrahedrally coordinated cation encapsulated by 12 additional metal octahedra that are bridged through OH^- or O^{2-} groups. The exterior metal cations can connect via shared edges or corners, which leads to five different isomeric (α, β, γ, δ, and ε) forms. The chemical diversity for anionic POMs is vast, with the five Keggin isomers formed by octahedrally coordinated V, Mo, W, Nb, and Ta ions incapsulating P, Si, Ge, or As cations.[2] Structural topologies associated with cationic aluminum-based POMs are notably less diverse, with over 90% of the known species related to the δ-, and ε-Keggin topology cations. Chemical diversity for the cationic aluminum POMs are also much more limited than what is observed for the anionic species, with only Ga^{3+} and Ge^{4+} full substitution reported for the tetrahedral position and Ga^{3+} and Cr^{3+} partial substitution reported in octahedral position.[3-6] The chemical diversity of the Keggin-topology and the reactivity of these nanoscale clusters has resulted in their use within industrial catalysis and water purification.[7-9] Additional efforts are ongoing to explore their use as metallodrugs for cancer treatement[10], electrodes for Li^+ batteries and energy storage[11-12], multifunctional sensor[13] and redox-based nonvolatile memory materials[14]. The metal oxo Keggin clusters containing aluminum, iron and others have also been found in natural systems and believe to control different geochemical processes.[15-17]

Keggin isomers can also undergo additional hydrolysis reactions or coordination with linkers that result in the formation of larger (>1 nm) oligomers. For the anionic POMs, formation of lacunary structures based upon the α- and β-Keggin motif results in the formation of these larger clusters, with the Wells-Dawson topology as a well-known example. Additional linkages occur through use of either organic linkers[18] or octahedral/heteroatom substitution[18] to create an array of larger anionic POMs based upon two to four Keggin clusters. For polyaluminum Keggin cations, the δ-isomer is the only known synthon and either condenses to form the Al_{26} species or bridges through additional aluminum octahedra to create only two additional topologies (Al_{30} or Al_{32}).[19-20] Currently, the largest known cationic POM topologies contains only contains two Keggin units and reflects a lack of understanding on the condensation process within the Al^{3+} system.

Previous studies have demonstrated that heteroatom substitution is important for the oligomerization process and can lead to a new understanding of the condensation process for cationic POMs. For example, Mothé-Esteves *et al*., indicated that octahedral substitution in Keggin units within anionic POMs can enhance formation of reversible H-bond with other units, which further can condensate into bridging oxygen bond between two metals.[21] This strategy has been employed to synthesize trimers [22-23] and tetramers[24-30] of lacunary or tri-lacunary Keggin units within polyanionic

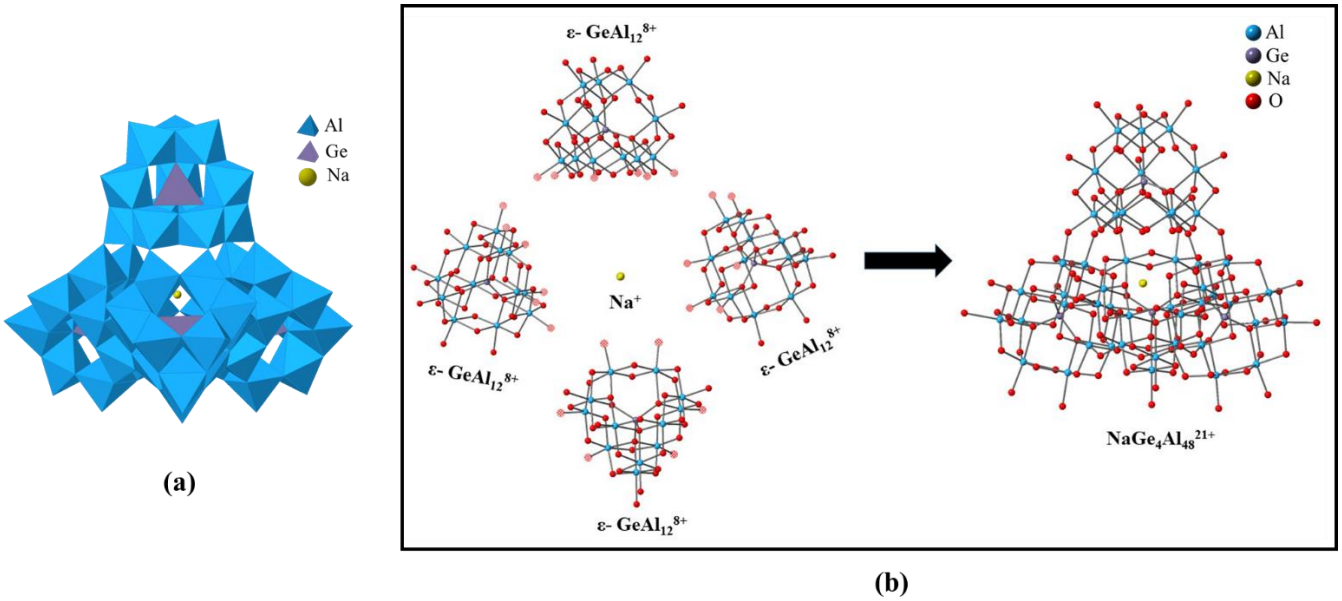

Figure 1. (a) Polyhedra representation of $NaGe_4Al_{48}^{21+}$ Keggin cluster with Al^{3+}, Ge^{4+} and Na^+ represented in blue, purple, and yellow, respectively. (b) Ball and stick representation for the formation of $NaGe_4\mathbf{Al_{48}^{+21}}$ from individual ε-$GeAl_{12}^{8+}$ building block. The surface H_2O groups that have undergone self-condensation are depicted by translucent red spheres.

POMs. In the case of cationic systems, previous computational work[31] and experimental observations[32-33] demonstrated that tetrahedral heteroatom substitution at center of Al_{13}^{7+} Keggin can tune the chemical behavior of terminal H_2O groups attached to octahedral metal ions. This surface reactivity is vital to the condensation process and may be utilized as synthetic strategy in Al^{3+} Keggin systems to generate larger POMs with novel chemical properties.

In the present study, we describe the synthesis and characterization of a giant (~2.4 nm) Keggin-type aluminum oxo polycation $[NaGe_4O_{16}Al_{48}(OH)_{108}(H_2O)_{24}]^{21+}$ (**Ge_4Al_{48}**) composed of four ε-$GeAl_{12}$ Keggin units, without the use of lacunary structures or organic linkers. Additional investigations of the solution phase using Dynamic Light Scattering (DLS) provides evidence of the larger cluster within the solution phase. Density Functional Theory (DFT) calculations also provide an energetic understanding of the formation pathway and additional insights into the role of the counterions in the hydrolysis and condensation processes.

The Ge_4Al_{48} cluster was synthesized by thermal aging of an aqueous solution containing Al^{3+} and Ge^{4+} cation. Initially, a mixed Al^{3+}/Ge^{4+} solution was partially hydrolyzed at 80 °C, which is the standard procedure for forming the $[GeO_4Al_{12}OH_{24}H_2O_{12})]^{8+}$(ε-$GeAl_{12}$) Keggin.[4] Evaporation of the solution at this point with addition of selenate anions results in the crystallization of the $[GeO_4Al_{12}(OH)_{24}(H_2O)_{12}](SeO_4)_4$ •14 H_2O phase. Additional thermal aging of this solution at 90 °C for seven days, followed by addition of the 2,6- napthalenedisulfonate (2,6-NDS) ion yielded small, transparent crystals of $[NaGe_4O_{16}Al_{48}(OH)_{108}(H_2O)_{24}](2,6\text{-}NDS)_7Cl_7(H_2O)_{45}$ with approximate yields of 15% based on Al^{3+}.

Structural features of the solid-state material was analyzed using single crystal X-ray diffraction and indicated that the Ge_4Al_{48} cluster is based upon the ε-Keggin unit. Each ε-isomer is composed of a tetrahedral $Ge(O)_4$ unit surrounded by 12 $Al(OH)_6$ octahedra that are connected via edge-sharing μ_2-OH groups between $Al_3(OH)_6(H_2O)_3$ trimers (Fig. 1). The Ge-O bond distances ranged from 1.760(11) to 1.806(10) Å and are similar to the isolated ε-$GeAl_{12}^{8+}$ Keggin (Ge-O = 1.809(8) Å).[4] **Ge_4Al_{48}** is formed when four ε-$GeAl_{12}$ units are linked via twelve μ_2-OH bridging groups (two linkages per trimeric unit) in a tetrahedral (T_d) arrangement. A 0.9 nm cavity exists at the center of the **Ge_4Al_{48}** cluster, but X-ray diffraction could only identify a single Na^+ cation within this space. The $[Na(Ge_4Al_{48})]^{21+}$ unit is charge balanced by seven 2,6-napthalenedisulfonate and seven chloride ions for an overall compound formula of $[NaGe_4O_{16}Al_{48}(OH)_{108}(H_2O)_{24}](2,6\text{-}NDS)_7Cl_7(H_2O)_{45}$. The 2,6-napthalenedisulfonate ions are arranged within two separate channels in the [010] and [101] directions. These anions aid in the crystallization of the Ge_4Al_{48} cluster by engaging in both π–π interaction between the naphthalene rings and electrostatics with the positively charged clusters.[19]

The structural topology observed in **Ge_4Al_{48}** is unique because it is the only giant cationic tetrahedron formed through non-lacunary ε-isomers within the POM family of compounds. A handful of large tetrahedron forms have been reported for polyanions, but they only occurs through Dawson lacunary clusters[29-30, 34] or other lacunary fragments.[27-28, 35-36] Only one compound reported by Hussain *et al*. contains direct linkages between the β-Keggin isomer $[(\beta\text{-}Ti_2SiW_{10}O_{39})_4]^{24-}$ but forms a circular wheel instead of a larger tetrahedral unit.[37] The wheel also contains three K^+ ions, one present in the central cavity and another two act as "wheel caps". The presence of the Ti^{4+} cations as a surface reactive species was found to be key to the formation of this larger Keggin-based cluster as it provides an avenue for additional hydrolysis and condensation.

Additional chemical characterization of this system confirms the heteroatom content and the presence of the oligomerized **Ge_4Al_{48}** cluster in thermally aged solutions. Solid-state crystals were dissolved in an acidic solution and the elemental content was analyzed by ICP-MS. The theoretical Al:Ge ratio for the $Ge_4Al_{48}^{20+}$ cluster is 12 and our experimental value was 12.43± 0.45 (Table S1), which is within error of the expected value. Formation

of the $Ge_4Al_{48}^{20+}$ tetramer in solution was also supported by the hydrodynamic diameter measurement of Keggin ions by Dynamic Light Scattering (DLS) measurements (Fig. 2). The unaged, partially hydrolyzed Ge^{4+}/Al^{3+} stock solution displays one peak in the

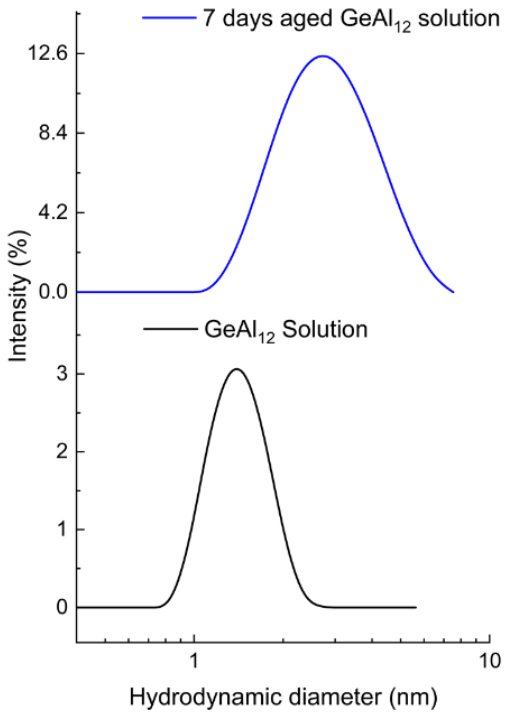

Figure 2. Particle size distribution from DLS of as prepared $GeAl_{12}$ solution and after aging 7 days at 90 °C.

DLS plot with a peak centroid at 1.2 nm. This value is consistent with the theoretical value for the size of ε-$GeAl_{12}$ cluster. Upon thermal aging, the single peak in the DLS plot broadens and shifts to a higher particle size. The peak centroid in the aged solutions is at 2.8 nanometers, which is now consistent with the formation of the $Ge_4Al_{48}^{20+}$ tetramer.

One important aspect of the formation of the $Ge_4Al_{48}^{20+}$ tetramer is the divergence from the previously studied Al^{3+} and Al^{3+}/Ga^{3+} systems.[5, 19] Oligomerization within these systems initially begins with the conversion of the ε-Keggin form to the δ-isomer. Previous studies have postulated that rotated trimer of the δ-Al_{13} and δ-$GaAl_{12}$ is a reactive site, which can form larger clusters by self-condensation μ_2-OH bridging or use of additional Al^{3+} octahedra to link fragments together.[5, 19] In the Al^{3+}/Ge^{4+} system there is no experimental evidence for the formation of the δ-isomer and the $Ge_4Al_{48}^{20+}$ tetramer offers the glimpse into the structural features of the condensation product within this system. Our initial hypotheses regarding the formation of the $Ge_4Al_{48}^{20+}$ tetramer is that the ε-$GeAl_{12}$ synthon has reactive terminal H_2O groups that allow for condensation into $Ge_4Al_{48}^{20+}$. We use Density Functional Theory (DFT) calculations to test this hypothesis and provide additional insights into the system.

The surface reactivity of the ε- and δ-isomers for Al_{13} and $GeAl_{12}$ clusters was investigated to further evaluate the condensation process. We have previously used modeled outer-sphere adsorption of sulfate as a probe of cluster surface reactivity. In some cases, the adsorption leads to the deprotonation of different surface sites over the course of geometry optimization, thus identifying relatively labile protons While sulfate anions are not present in the thermally aged solution, they are effective as a probe adsorbate to identify the most acidic proton that can act as the driving force for the formation of this tetramer. This modeling approach has been applied to the δ-$GaAl_{12}$ cluster, where it was used to establish that the driving force for oligomerization is deprotonation of the rotated trimer.[5] Here, we again use modeled adsorption with a sulfate probe to study how Ge^{4+} substitution effects on surface reactivity (in terms of adsorption energies and ease of deprotonation) of the ε and δ-isomers for the Al_{13} and $GeAl_{12}$ and the formation of $Ge_4Al_{48}^{20+}$ (additional details in SI).

We model sulfate-cluster interactions starting from two chemically-distinct starting configurations (referred to as Sites 1 and 2) for ε-Al_{13} and ε-$GeAl_{12}$ Keggin clusters (Fig. 3b). In Site 1, the anion is positioned to interact with two terminal η_1-H_2O groups on two different $Al_3(OH)_6(H_2O)_3$ trimers, corresponding to point where the ε-$GeAl_{12}$ Keggin clusters oligomerize into the $Ge_4Al_{48}^{20+}$ tetramer. In Site 2, the sulfate anion can engage with a mixture of η_1-H_2O and μ_2-OH groups on the surface of one $Al_3(OH)_6(H_2O)_3$ trimer unit. We compare changes in the Mulliken population (Δq_m) to deprotonation events. Of the four ε-Keggin interactions, only Site 1 sulfate interactions with ε-$GeAl_{12}$ (Table S2 and Figure 2) result in deprotonation and a Δq_m value greater than 0.50 e. All other interactions have Δq_m values of less than 0.50 e and did not exhibit deprotonation, similar to previous observations on Keggin-anion interactions.[5, 31, 38]

To bridge the understanding between isomers and heteroatom identity with regard to condensation reactions, we also assessed the δ-isomers for $GeAl_{12}$ and Al_{13} using the sulfate anion as our probe adsorbate (Table S3 and Figure S1). The ε-isomer has four equivalent edge-sharing trimers whereas the δ-isomer has three edge-sharing trimers and one rotated, corner-sharing trimer. The number of corner- versus edge-trimers influences the surface reactivity of the nanocluster. For the δ-isomer, three chemically distinct sites can be found on Keggin surface that correspond to interactions with η_1-H_2O and μ_2-OH groups on the different $Al_3(OH)_6(H_2O)_3$ units. For δ-Al_{13}, deprotonation only occurs associated with the reactive trimer (rotated $Al_3(OH)_6(H_2O)_3$ group), whereas higher charge transfer and deprotonation is observed for all sites on the δ-$GeAl_{12}$ clusters (Table S3). Our calculation confirms that deprotonation events for the reactive site on the δ-Al_{13} leads to the formation of Al_{26}, Al_{30} or Al_{32}. However, the high charge transfer on all surface sites associate the δ-$GeAl_{12}$ cluster suggests that random condensation will occur and likely form amorphous precipitates.

In summary, we have reported the synthesis and characterization of a new cationic POM tetramer ($Ge_4Al_{48}^{20+}$) composed solely of ε-Keggin units without any lacunary features or organic linkers. DLS experiments indicate that this large tetramer occurs in partially hydrolyzed solutions containing Al^{3+} and Ge^{4+} after thermal aging for seven days. DFT calculations indicated that Ge^{4+} substitution at the central tetrahedral site of the Keggin topology is key to the formation of the tetramer because it specifically deprotonates η_1-H_2O to form symmetric μ_2-OH bridges, which can be linked to the formation of the tetramer. This work has demonstrated the importance of the metal cation identity to control stability and reactivity, even when it is located at the center of the Keggin cluster. More broadly, it provides additional details in the nucleation process of metal oxide and hydroxide phases from POM synthons that can be used to provide additional controls on the development of functional materials.

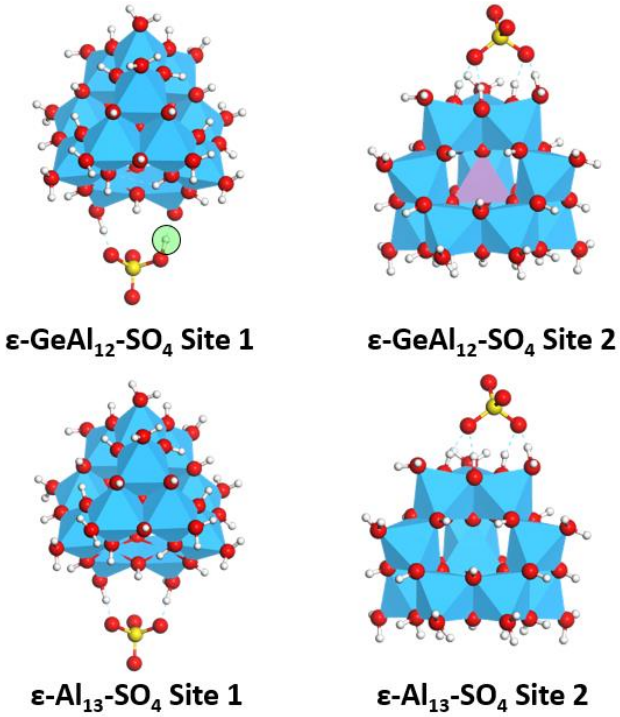

Figure 3. Different surface sites of ε- $GeAl_{12}$ and ε- Al_{13} interacting with SO_4^{2-} ion. The abstracted proton is highlighted with a green circle. Blue and purple polyhedra are used to represent Al and Ge atoms, respectively. Red, yellow and white balls are used to represent O, S, and H atoms, respectively.

ASSOCIATED CONTENT

Supporting Information

A supporting information file in pdf format is available free of charge on the ACS Publications website (http://pubs.acs.org). The supporting information file contains experimental details, result of elemental analysis, result of computational calculation and additional figures. Additional crystallographic information files can be found on the Cambridge Structural Database by requesting deposition numbers 2027043.

AUTHOR INFORMATION

Corresponding Author

*Tori Z. Forbes: tori-forbes@uiowa.edu

Author Contributions

TZF and SEM provided resources, support and funding to carry-out the study. MS and JAS did the synthesis experiment. MS did all the chemical characterization, crystallography and experimental data analysis. JLB conducted all of the DFT calculations. MS and JLB prepared the initial draft of manuscript. All authors contributed to the writing and editing of final manuscript for the submission.

Notes

The authors declare no competing financial interests.

ACKNOWLEDGMENT

SEM acknowledges computational resources provided by the University of Iowa. This work used the Extreme Science and Engineering Discovery Environment (XSEDE),[39] which is supported by the National Science Foundation grant number ACI-1548562 though allocation TG-GEO160006. We acknowledge Prof. Aliasger Salem and Dr. Lr Jaidev Chakka (UI college of Pharmacy) for their help regarding DLS experiment. TZF and MS also acknowledge American Crystallographic Association (ACA) summer school 2019 at Northwestern University for their travel support to teach MS advanced-level crystallography. JLB acknowledges support from the University of Iowa's Dissertation Writing Fellowship.

REFERENCES

1. Keggin, J. F., Structure of the Molecule of 12-Phosphotungstic Acid. *Nature* **1933,** *131* (3321), 908-909.
2. Li, D.; Ma, P.; Niu, J.; Wang, J., Recent advances in transition-metal-containing Keggin-type polyoxometalate-based coordination polymers. *Coordination Chemistry Reviews* **2019,** *392*, 49-80.
3. Parker, W. O. N.; Millini, R.; Kiricsi, I., Metal Substitution in Keggin-Type Tridecameric Aluminum−Oxo−Hydroxy Clusters. *Inorganic Chemistry* **1997,** *36* (4), 571-575.
4. Lee, A. P.; Phillips, B. L.; Olmstead, M. M.; Casey, W. H., Synthesis and Characterization of the GeO4Al12(OH)24(OH2)128+ Polyoxocation. *Inorganic Chemistry* **2001,** *40* (17), 4485-4487.
5. Shohel, M.; Bjorklund, J. L.; Ovrom, E. A.; Mason, S. E.; Forbes, T. Z., Ga3+ Incorporation into Al13 Keggin Polyoxometalates and the Formation of δ-(GaAl12)7+ and (Ga2.5Al28.5)19+ Polycations. *Inorganic Chemistry* **2020,** *59* (15), 10461-10472.
6. Wang, W.; Fullmer, L. B.; Bandeira, N. A. G.; Goberna-Ferrón, S.; Zakharov, L. N.; Bo, C.; Keszler, D. A.; Nyman, M., Crystallizing Elusive Chromium Polycations. *Chem* **2016,** *1* (6), 887-901.

7. Muñoz, M.; Romanelli, G.; Botto, I. L.; Cabello, C. I.; Lamonier, C.; Capron, M.; Baranek, P.; Blanchard, P.; Payen, E., Al13–[X–Mo/WOn] (X=Al, Co, V, P) composites as catalysts in clean oxidation of aromatic sulfides. *Applied Catalysis B: Environmental* **2010,** *100* (1), 254-263.
8. Benito, I.; del Riego, A.; Martínez, M.; Blanco, C.; Pesquera, C.; González, F., Toluene methylation on Al13- and GaAl12-pillared clay catalysts. *Applied Catalysis A: General* **1999,** *180* (1), 175-182.
9. Stewart, T. A.; Trudell, D. E.; Alam, T. M.; Ohlin, C. A.; Lawler, C.; Casey, W. H.; Jett, S.; Nyman, M., Enhanced Water Purification: A Single Atom Makes a Difference. *Environmental Science & Technology* **2009,** *43* (14), 5416-5422.
10. Bijelic, A.; Aureliano, M.; Rompel, A., Polyoxometalates as Potential Next-Generation Metallodrugs in the Combat Against Cancer. *Angewandte Chemie International Edition* **2019,** *58* (10), 2980-2999.
11. Yeo, H. J.; Paik, Y.; Paek, S.-M.; Honma, I., Keggin-type aluminum polyoxocation/graphene oxide hybrid as a new nanostructured electrode for a lithium ion battery. *Journal of Physics and Chemistry of Solids* **2012,** *73* (12), 1417-1419.
12. Priyadarshini, M.; Shanmugan, S.; Kirubakaran, K. P.; Thomas, A.; Prakash, M.; Senthil, C.; Lee, C. W.; Vediappan, K., High energy storage of Li-ions on keggin-type polyoxometalate as electrodes for rechargeable lithium batteries. *Journal of Physics and Chemistry of Solids* **2020,** *142*, 109468.
13. Wang, G.; Zhou, J.; Li, J., Layer-by-layer self-assembly aluminum Keggin ions/Prussian blue nanoparticles ultrathin films towards multifunctional sensing applications. *Biosensors and Bioelectronics* **2007,** *22* (12), 2921-2925.
14. Chen, X.; Huang, P.; Zhu, X.; Zhuang, S.; Zhu, H.; Fu, J.; Nissimagoudar, A. S.; Li, W.; Zhang, X.; Zhou, L.; Wang, Y.; Lv, Z.; Zhou, Y.; Han, S.-T., Keggin-type polyoxometalate cluster as an active component for redox-based nonvolatile memory. *Nanoscale Horizons* **2019,** *4* (3), 697-704.
15. Furrer, G.; Phillips, B. L.; Ulrich, K.-U.; Pöthig, R.; Casey, W. H., The Origin of Aluminum Flocs in Polluted Streams. *Science* **2002,** *297* (5590), 2245.
16. Sadeghi, O.; Zakharov, L. N.; Nyman, M., Aqueous formation and manipulation of the iron-oxo Keggin ion. *Science* **2015,** *347* (6228), 1359.
17. Nyman, M., Polyoxometalates and Other Metal-Oxo Clusters in Nature. In *Encyclopedia of Geochemistry: A Comprehensive Reference Source on the Chemistry of the Earth*, White, W. M., Ed. Springer International Publishing: Cham, 2016; pp 1-5.
18. Long, D.-L.; Burkholder, E.; Cronin, L., Polyoxometalate clusters, nanostructures and materials: From self assembly to designer materials and devices. *Chemical Society Reviews* **2007,** *36* (1), 105-121.
19. Abeysinghe, S.; Unruh, D. K.; Forbes, T. Z., Crystallization of Keggin-Type Polyaluminum Species by Supramolecular Interactions with Disulfonate Anions. *Crystal Growth & Design* **2012,** *12* (4), 2044-2051.
20. Sun, Z.; Wang, H.; Tong, H.; Sun, S., A Giant Polyaluminum Species S−Al32 and Two Aluminum Polyoxocations Involving Coordination by Sulfate Ions S−Al32 and S−K−Al13. *Inorganic Chemistry* **2011,** *50* (2), 559-564.
21. Mothé-Esteves, P.; Pereira, M. M.; Arichi, J.; Louis, B., How Keggin-Type Polyoxometalates Self-Organize into Crystals. *Crystal Growth & Design* **2010,** *10* (1), 371-378.
22. Matsunaga, S.; Inoue, Y.; Mihara, K.; Nomiya, K., Synthesis and crystal structure of hexacerium(IV) cluster-containing Keggin polyoxometalate trimer. *Inorganic Chemistry Communications* **2017,** *80*, 61-64.
23. Al-Kadamany, G. A.; Hussain, F.; Mal, S. S.; Dickman, M. H.; Leclerc-Laronze, N.; Marrot, J.; Cadot, E.; Kortz, U., Cyclic Ti9 Keggin Trimers with Tetrahedral (PO4) or Octahedral (TiO6) Capping Groups. *Inorganic Chemistry* **2008,** *47* (19), 8574-8576.
24. Sakai, Y.; Yoza, K.; Kato, C. N.; Nomiya, K., Tetrameric, Trititanium(IV)-Substituted Polyoxotungstates with an α-Dawson Substructure as Soluble Metal-Oxide Analogues: Molecular Structure of the Giant "Tetrapod" [(α-1,2,3-P2W15Ti3O62)4{μ3-Ti(OH)3}4Cl]45−. *Chemistry – A European Journal* **2003,** *9* (17), 4077-4083.
25. Sakai, Y.; Ohta, S.; Shintoyo, Y.; Yoshida, S.; Taguchi, Y.; Matsuki, Y.; Matsunaga, S.; Nomiya, K., Encapsulation of Anion/Cation in the Central Cavity of Tetrameric Polyoxometalate, Composed of Four Trititanium(IV)-Substituted α-Dawson Subunits, Initiated by Protonation/Deprotonation of the Bridging Oxygen Atoms on the Intramolecular Surface. *Inorganic Chemistry* **2011,** *50* (14), 6575-6583.
26. Zhang, Z.; Wang, Y.-L.; Yang, G.-Y., An unprecedented Zr-containing polyoxometalate tetramer with mixed trilacunary/dilacunary Keggin-type polyoxotungstate units. *Acta Crystallographica Section C Structural Chemistry* **2018,** *74* (11), 1284-1288.
27. Zhao, J.-W.; Zhang, J.; Zheng, S.-T.; Yang, G.-Y., Combination of Lacunary Polyoxometalates and High-Nuclear Transition-Metal Clusters under Hydrothermal Conditions. 5. A Novel Tetrameric Cluster of [{FeIIFeIII12(μ3-OH)12(μ4-PO4)4}(B-α-PW9O34)4]22. *Inorganic Chemistry* **2007,** *46* (26), 10944-10946.
28. Wang, K.-Y.; Bassil, B. S.; Lin, Z.-G.; Haider, A.; Cao, J.; Stephan, H.; Viehweger, K.; Kortz, U., Ti7-containing, tetrahedral 36-tungsto-4-arsenate(iii) [Ti6(TiO6)(AsW9O33)4]20−. *Dalton Transactions* **2014,** *43* (43), 16143-16146.
29. Pradeep, C. P.; Long, D.-L.; Kögerler, P.; Cronin, L., Controlled assembly and solution observation of a 2.6 nm polyoxometalate 'super' tetrahedron cluster: [KFe12(OH)18(α-1,2,3-P2W15O56)4]29−. *Chemical Communications* **2007,** (41), 4254-4256.
30. Yoshitaka, S.; Shoko, Y.; Takeshi, H.; Hideyuki, M.; Kenji, N., Tetrameric, Tri-Titanium(IV)-Substituted Polyoxometalates with an α-Dawson Substructure as Soluble Metal Oxide Analogues. Synthesis and Molecular Structure of Three Giant "Tetrapods" Encapsulating Different Anions (Br−, I−, and NO3−). *Bulletin of the Chemical Society of Japan* **2007,** *80* (10), 1965-1974.
31. Bjorklund, J. L.; Bennett, J. W.; Forbes, T. Z.; Mason, S. E., Modeling of MAl12 Keggin Heteroatom Reactivity by Anion Adsorption. *Crystal Growth & Design* **2019,** *19* (5), 2820-2829.
32. Lee, A. P.; Furrer, G.; Casey, W. H., On the Acid–Base Chemistry of the Keggin Polymers: GaAl12 and GeAl12. *Journal of Colloid and Interface Science* **2002,** *250* (1), 269-270.
33. Lee, A. P.; Phillips, B. L.; Casey, W. H., The kinetics of oxygen exchange between the GeO4Al12(OH)24(OH2)128+(aq) molecule and aqueous solutions. *Geochimica et Cosmochimica Acta* **2002,** *66* (4), 577-587.
34. Sakai, Y.; Yoza, K.; Kato, C. N.; Nomiya, K., A first example of polyoxotungstate-based giant molecule. Synthesis and molecular structure of a tetrapod-shaped Ti–O–Ti bridged anhydride form of Dawson tri-titanium(iv)-substituted polyoxotungstate. *Dalton Transactions* **2003,** (18), 3581-3586.
35. Al-Kadamany, G. Synthesis, Structure and Catalytic Activity of Titanium, Zirconium and Hafnium-Containing Polyoxometalates. Jacobs University, IRC-Library, Information Resource Center der Jacobs University Bremen, 2010.
36. Kim, G.-S.; Zeng, H.; VanDerveer, D.; Hill, C. L., A Supramolecular Tetra-Keggin Polyoxometalate [Nb4O6(α-Nb3SiW9O40)4]20− *Angewandte Chemie International Edition* **1999,** *38* (21), 3205-3207.
37. Hussain, F.; Bassil, B. S.; Bi, L.-H.; Reicke, M.; Kortz, U., Structural Control on the Nanomolecular Scale: Self-Assembly of the Polyoxotungstate Wheel [{β-Ti2SiW10O39}4]24−. *Angewandte Chemie International Edition* **2004,** *43* (26), 3485-3488.
38. Bennett, J. W.; Bjorklund, J. L.; Forbes, T. Z.; Mason, S. E., Systematic Study of Aluminum Nanoclusters and Anion Adsorbates. *Inorganic Chemistry* **2017,** *56* (21), 13014-13028.
39. John Towns, T. C., Maytal Dahan, Ian Foster, Kelly Gaither, Andrew Grimshaw, Victor Hazlewood, Scott Lathrop, Dave Lifka, Gregory D. Peterson, Ralph Roskies, J. Ray Scott, Nancy Wilkins-Diehr, XSEDE: Accelerating Scientific Discovery. *Computing in Science & Engineering* **2014,** *16* (5), 62-74.

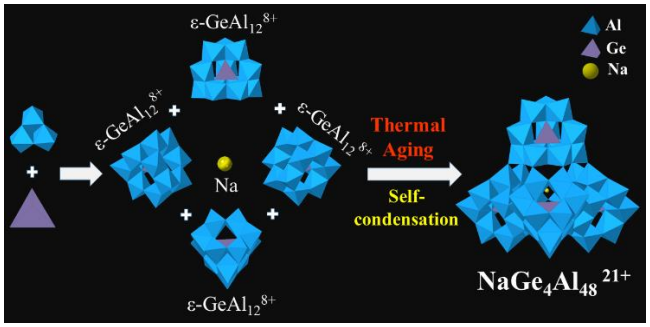

The proposed mechanism for the formation of tetrameric $Na[Ge_4O_{16}Al_{48}(OH)_{108}(H_2O)_{24}]^{20+}$ ($NaGe_4Al_{48}^{21+}$) resulting from self-condensation of ε-$GeAl_{12}^{8+}$ upon thermal aging.

Formation of the $[Ge_4O_{16}Al_{48}(OH)_{108}(H_2O)_{24}]^{20+}$ tetramer from condensation of ε-$GeAl_{12}$ Keggin polycations

Mohammad Shohel, Jennifer L. Bjorklund, Jack A. Smith, Sara E. Mason, Tori Z. Forbes*

Department of Chemistry, University of Iowa, Iowa City, IA-52242
*Corresponding author: tori-forbes@uiowa.edu_

Supporting Information Placeholder

ABSTRACT: Keggin-type polyaluminum cations belong to a unique class of polyoxometalates (POMs) with their large positive charge, hydroxo bridges, and divergent isomerization/oligomerization. Previously reported oligomerizations of the polyaluminum cations were driven solely by the δ-Keggin isomer, which created Al_{26}, Al_{30}, and Al_{32} dimeric species. We herein report the isolation of largest ever Keggin-type structure for this system through a unique mode of self-condensation among four ε-$GeAl_{12}^{8+}$ to form $[NaGe_4O_{16}Al_{48}(OH)_{108}(H_2O)_{24}]^{21+}$ (**Ge_4Al_{48}**). Elemental analysis confirms the Ge^{4+} substitution, and dynamic light scattering experiments indicated that these larger species exist in the thermally aged solutions. DFT calculations have revealed that a single atom Ge substitution in tetrahedral site of ε-Al_{13}^{7+} is the key for the formation this cluster because it activates the deprotonation at certain octahedral sites to assist self-condensation in a specific mode.

Since the discovery of Keggin-type polyoxometalates (POMs) in 1933,[1] chemists and material scientists have been fascinated by their unique structural features and applications in energy, medicine, and water purification. The Keggin topology was first identified as a phosphotungstate and contains a central tetrahedrally coordinated cation encapsulated by 12 additional metal octahedra that are bridged through OH^- or O^{2-} groups. The exterior metal cations can connect via shared edges or corners, which leads to five different isomeric (α, β, γ, δ, and ε) forms. The chemical diversity for anionic POMs is vast, with the five Keggin isomers formed by octahedrally coordinated V, Mo, W, Nb, and Ta ions incapsulating P, Si, Ge, or As cations.[2] Structural topologies associated with cationic aluminum-based POMs are notably less diverse, with over 90% of the known species related to the δ-, and ε-Keggin topology cations. Chemical diversity for the cationic aluminum POMs are also much more limited than what is observed for the anionic species, with only Ga^{3+} and Ge^{4+} full substitution reported for the tetrahedral position and Ga^{3+} and Cr^{3+} partial substitution reported in octahedral position.[3-6] The chemical diversity of the Keggin-topology and the reactivity of these nanoscale clusters has resulted in their use within industrial catalysis and water purification.[7-9] Additional efforts are ongoing to explore their use as metallodrugs for cancer treatement[10], electrodes for Li^+ batteries and energy storage[11-12], multifunctional sensor[13] and redox-based nonvolatile memory materials[14]. The metal oxo Keggin clusters containing aluminum, iron and others have also been found in natural systems and believe to control different geochemical processes.[15-17]

Keggin isomers can also undergo additional hydrolysis reactions or coordination with linkers that result in the formation of larger (>1 nm) oligomers. For the anionic POMs, formation of lacunary structures based upon the α- and β-Keggin motif results in the formation of these larger clusters, with the Wells-Dawson topology as a well-known example. Additional linkages occur through use of either organic linkers[18] or octahedral/heteroatom substitution[18] to create an array of larger anionic POMs based upon two to four Keggin clusters. For polyaluminum Keggin cations, the δ-isomer is the only known synthon and either condenses to form the Al_{26} species or bridges through additional aluminum octahedra to create only two additional topologies (Al_{30} or Al_{32}).[19-20] Currently, the largest known cationic POM topologies contains only contains two Keggin units and reflects a lack of understanding on the condensation process within the Al^{3+} system.

Previous studies have demonstrated that heteroatom substitution is important for the oligomerization process and can lead to a new understanding of the condensation process for cationic POMs. For example, Mothé-Esteves *et al*., indicated that octahedral substitution in Keggin units within anionic POMs can enhance formation of reversible H-bond with other units, which further can condensate into bridging oxygen bond between two metals.[21] This strategy has been employed to synthesize trimers [22-23] and tetramers[24-30] of lacunary or tri-lacunary Keggin units within polyanionic

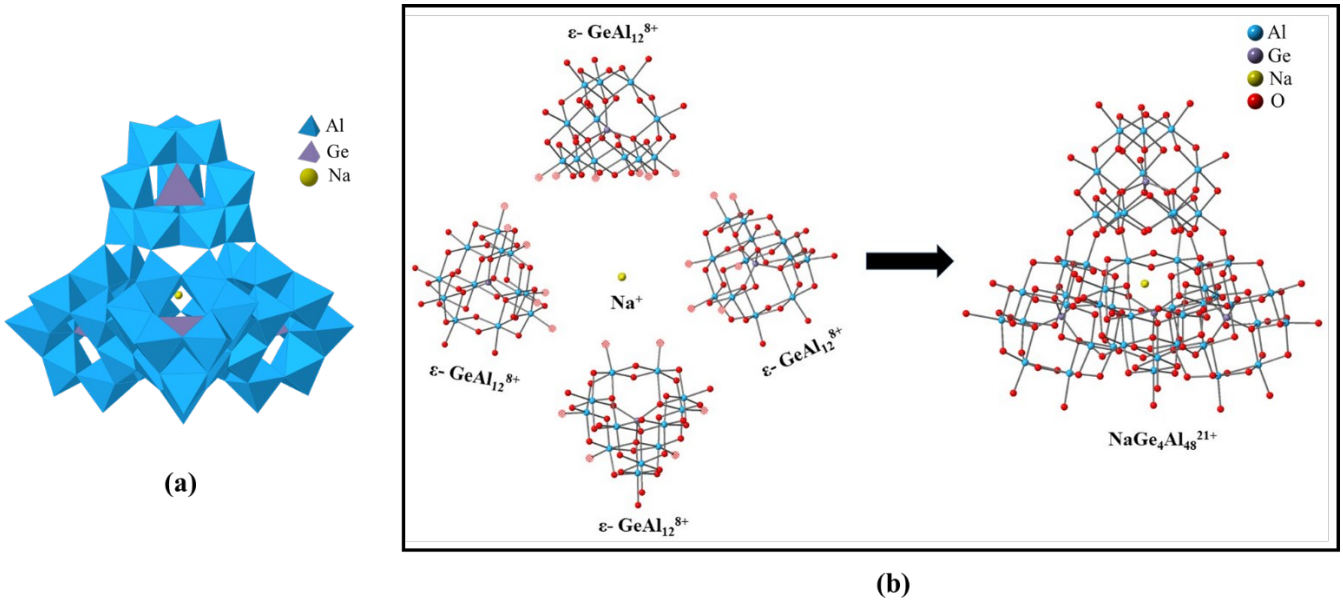

Figure 1. (a) Polyhedra representation of $NaGe_4Al_{48}^{21+}$ Keggin cluster with Al^{3+}, Ge^{4+} and Na^+ represented in blue, purple, and yellow, respectively. (b) Ball and stick representation for the formation of $NaGe_4$ Al_{48}^{+21} from individual ε-$GeAl_{12}^{8+}$ building block. The surface H_2O groups that have undergone self-condensation are depicted by translucent red spheres.

POMs. In the case of cationic systems, previous computational work[31] and experimental observations[32-33] demonstrated that tetrahedral heteroatom substitution at center of Al_{13}^{7+} Keggin can tune the chemical behavior of terminal H_2O groups attached to octahedral metal ions. This surface reactivity is vital to the condensation process and may be utilized as synthetic strategy in Al^{3+} Keggin systems to generate larger POMs with novel chemical properties.

In the present study, we describe the synthesis and characterization of a giant (~2.4 nm) Keggin-type aluminum oxo polycation $[NaGe_4O_{16}Al_{48}(OH)_{108}(H_2O)_{24}]^{21+}$ (**Ge_4Al_{48}**) composed of four ε-$GeAl_{12}$ Keggin units, without the use of lacunary structures or organic linkers. Additional investigations of the solution phase using Dynamic Light Scattering (DLS) provides evidence of the larger cluster within the solution phase. Density Functional Theory (DFT) calculations also provide an energetic understanding of the formation pathway and additional insights into the role of the counterions in the hydrolysis and condensation processes.

The Ge_4Al_{48} cluster was synthesized by thermal aging of an aqueous solution containing Al^{3+} and Ge^{4+} cation. Initially, a mixed Al^{3+}/Ge^{4+} solution was partially hydrolyzed at 80 °C, which is the standard procedure for forming the $[GeO_4Al_{12}OH_{24}H_2O_{12})]^{8+}$(ε-$GeAl_{12}$) Keggin.[4] Evaporation of the solution at this point with addition of selenate anions results in the crystallization of the $[GeO_4Al_{12}(OH)_{24}(H_2O)_{12}](SeO_4)_4 \cdot 14\ H_2O$ phase. Additional thermal aging of

this solution at 90 °C for seven days, followed by addition of the 2,6- napthalenedisulfonate (2,6-NDS) ion yielded small, transparent crystals of $[NaGe_4O_{16}Al_{48}(OH)_{108}(H_2O)_{24}](2,6\text{-}NDS)_7Cl_7(H_2O)_{45}$ with approximate yields of 15% based on Al^{3+}.

Structural features of the solid-state material was analyzed using single crystal X-ray diffraction and indicated that the Ge_4Al_{48} cluster is based upon the ε-Keggin unit. Each ε-isomer is composed of a tetrahedral $Ge(O)_4$ unit surrounded by 12 $Al(OH)_6$ octahedra that are connected via edge-sharing μ_2-OH groups between $Al_3(OH)_6(H_2O)_3$ trimers (Fig. 1). The Ge-O bond distances ranged from 1.760(11) to 1.806(10) Å and are similar to the isolated ε-$GeAl_{12}^{8+}$ Keggin (Ge-O = 1.809(8) Å).[4] **Ge_4Al_{48}** is formed when four ε-$GeAl_{12}$ units are linked via twelve μ_2-OH bridging groups (two linkages per trimeric unit) in a tetrahedral (T_d) arrangement. A 0.9 nm cavity exists at the center of the **Ge_4Al_{48}** cluster, but X-ray diffraction could only identify a single Na^+ cation within this space. The $[Na(Ge_4Al_{48})]^{21+}$ unit is charge balanced by seven 2,6-napthalenedisulfonate and seven chloride ions for an overall compound formula of $[NaGe_4O_{16}Al_{48}(OH)_{108}(H_2O)_{24}](2,6\text{-}NDS)_7Cl_7(H_2O)_{45}$. The 2,6-napthalenedisulfonate ions are arranged within two separate channels in the [010] and [101] directions. These anions aid in the crystallization of the Ge_4Al_{48} cluster by engaging in both π−π interaction between the naphthalene rings and electrostatics with the positively charged clusters.[19]

The structural topology observed in **Ge_4Al_{48}** is unique because it is the only giant cationic tetrahedron formed through non-lacunary ε-isomers within the POM family of compounds. A handful of large tetrahedron forms have been reported for polyanions, but they only occurs through Dawson lacunary clusters[29-30, 34] or other lacunary fragments.[27-28, 35-36] Only one compound reported by Hussain *et al*. contains direct linkages between the β-Keggin isomer $[(\beta\text{-}Ti_2SiW_{10}O_{39})_4]^{24-}$ but forms a circular wheel instead of a larger tetrahedral unit.[37] The wheel also contains three K^+ ions, one present in the central cavity and another two act as “wheel caps”. The presence of the Ti^{4+} cations as a surface reactive species was found to be key to the formation of this larger Keggin-based cluster as it provides an avenue for additional hydrolysis and condensation.

Additional chemical characterization of this system confirms the heteroatom content and the presence of the oligomerized **Ge_4Al_{48}** cluster in thermally aged solutions. Solid-state crystals were dissolved in an acidic solution and the elemental content was analyzed by ICP-MS. The theoretical Al:Ge ratio for the $Ge_4Al_{48}^{20+}$ cluster is 12 and our experimental value was 12.43± 0.45 (Table S1), which is within error of the expected value. Formation of the $Ge_4Al_{48}^{20+}$ tetramer in solution was also supported by the hydrodynamic diameter measurement of Keggin ions by Dynamic Light Scattering (DLS) measurements (Fig. 2). The unaged, partially hydrolyzed Ge^{4+}/Al^{3+} stock solution displays one peak in the

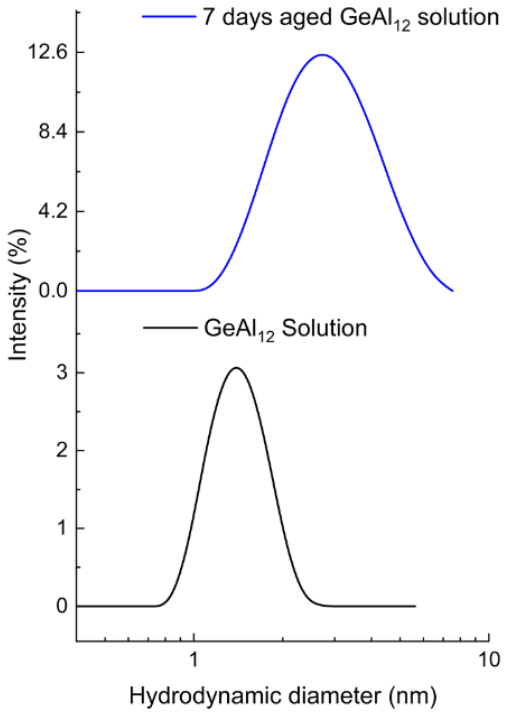

Figure 2. Particle size distribution from DLS of as prepared $GeAl_{12}$ solution and after aging 7 days at 90 °C.

DLS plot with a peak centroid at 1.2 nm. This value is consistent with the theoretical value for the size of ε-$GeAl_{12}$ cluster. Upon thermal aging, the single peak in the DLS plot broadens and shifts to a higher particle size. The peak centroid in the aged solutions is at 2.8 nanometers, which is now consistent with the formation of the $Ge_4Al_{48}^{20+}$ tetramer.

One important aspect of the formation of the $Ge_4Al_{48}^{20+}$ tetramer is the divergence from the previously studied Al^{3+} and Al^{3+}/Ga^{3+} systems.[5, 19] Oligomerization within these systems initially begins with the conversion of the ε-Keggin form to the δ-isomer. Previous studies have postulated that rotated trimer of the δ-Al_{13} and δ-$GaAl_{12}$ is a reactive site, which can form larger clusters by self-condensation μ_2-OH bridging or use of additional Al^{3+} octahedra to link fragments together.[5, 19] In the Al^{3+}/Ge^{4+} system there is no experimental evidence for the formation of the δ-isomer and the $Ge_4Al_{48}^{20+}$ tetramer offers the glimpse into the structural features of the condensation product within this system. Our initial hypotheses regarding the formation of the $Ge_4Al_{48}^{20+}$ tetramer is that the ε-$GeAl_{12}$ synthon has reactive terminal H_2O groups that allow for condensation into $Ge_4Al_{48}^{20+}$. We use Density Functional Theory (DFT) calculations to test this hypothesis and provide additional insights into the system.

The surface reactivity of the ε- and δ-isomers for Al_{13} and $GeAl_{12}$ clusters was investigated to further evaluate the condensation process. We have previously used modeled outer-sphere adsorption of sulfate as a probe of cluster surface reactivity. In some cases, the adsorption leads to the deprotonation of different surface sites over the course of geometry optimization, thus identifying relatively labile protons While sulfate anions are not present in the thermally aged solution, they are effective as a probe adsorbate to identify the most acidic proton that can act as the driving force for the formation of this tetramer. This modeling approach has been applied to the δ-$GaAl_{12}$ cluster, where it was used to establish that the driving force for oligomerization is deprotonation of the rotated trimer.[5] Here, we again use modeled adsorption with a sulfate probe to study how Ge^{4+} substitution effects on surface reactivity (in terms of adsorption energies and ease of deprotonation) of the ε and δ-isomers for the Al_{13} and $GeAl_{12}$ and the formation of $Ge_4Al_{48}^{20+}$ (additional details in SI).

We model sulfate-cluster interactions starting from two chemically-distinct starting configurations (referred to as Sites 1 and 2) for ε-Al_{13} and ε-$GeAl_{12}$ Keggin clusters (Fig. 3b). In Site 1, the anion is positioned to interact with two terminal η_1-H_2O groups on two different $Al_3(OH)_6(H_2O)_3$ trimers, corresponding to point where the ε-$GeAl_{12}$ Keggin clusters oligomerize into the $Ge_4Al_{48}^{20+}$ tetramer. In Site 2, the sulfate anion can engage with a mixture of η_1-H_2O and μ_2-OH groups on the surface of one $Al_3(OH)_6(H_2O)_3$ trimer unit. We compare changes in the Mulliken population (Δq_m) to deprotonation events. Of the four ε-Keggin interactions, only Site 1 sulfate interactions with ε-$GeAl_{12}$ (Table S2 and Figure 2) result in deprotonation and a Δq_m value greater than 0.50 e. All other interactions have Δq_m values of less than 0.50 e and did not exhibit deprotonation, similar to previous observations on Keggin-anion interactions.[5, 31, 38]

To bridge the understanding between isomers and heteroatom identity with regard to condensation reactions, we also assessed the δ-isomers for $GeAl_{12}$ and Al_{13} using the sulfate anion as our probe adsorbate (Table S3 and Figure S1). The ε-isomer has four equivalent edge-sharing trimers whereas the δ-isomer has three edge-sharing trimers and one rotated, corner-sharing trimer. The number of corner- versus edge-trimers influences the surface reactivity of the nanocluster. For the δ-isomer, three chemically distinct sites can be found on Keggin surface that correspond to interactions with η_1-H_2O and μ_2-OH groups on the different $Al_3(OH)_6(H_2O)_3$ units. For δ-Al_{13}, deprotonation only occurs associated with the reactive trimer (rotated $Al_3(OH)_6(H_2O)_3$ group), whereas higher charge transfer and deprotonation is observed for all sites on the δ-$GeAl_{12}$ clusters (Table S3). Our calculation confirms that deprotonation events for the reactive site on the δ-Al_{13} leads to the formation of Al_{26}, Al_{30} or Al_{32}. However, the high charge transfer on all surface sites associate the δ-$GeAl_{12}$ cluster suggests that random condensation will occur and likely form amorphous precipitates.

In summary, we have reported the synthesis and characterization of a new cationic POM tetramer ($Ge_4Al_{48}^{20+}$) composed solely of ε-Keggin units without any lacunary features or organic linkers. DLS experiments indicate that this large tetramer occurs in partially hydrolyzed solutions containing Al^{3+} and Ge^{4+} after thermal aging for seven days. DFT calculations indicated that Ge^{4+} substitution at the central tetrahedral site of the Keggin topology is key to the formation of the tetramer because it specifically deprotonates η_1-H_2O to form symmetric μ_2-OH bridges, which can be linked to the formation of the tetramer. This work has demonstrated the importance of the metal cation identity to control stability and reactivity, even when it is located at the center of the Keggin cluster. More broadly, it provides additional details in the nucleation process of metal oxide and hydroxide phases from POM synthons that can be used to provide additional controls on the development of functional materials.

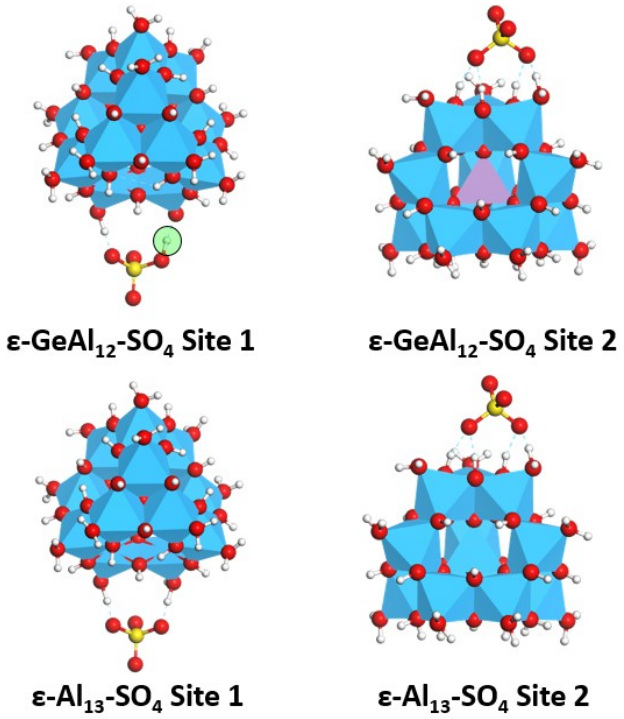

Figure 3. Different surface sites of ε- $GeAl_{12}$ and ε- Al_{13} interacting with SO_4^{2-} ion. The abstracted proton is highlighted with a green circle. Blue and purple polyhedra are used to represent Al and Ge atoms, respectively. Red, yellow and white balls are used to represent O, S, and H atoms, respectively.

ASSOCIATED CONTENT

Supporting Information

A supporting information file in pdf format is available free of charge on the ACS Publications website (http://pubs.acs.org). The supporting information file contains experimental details, result of elemental analysis, result of computational calculation and additional figures. Additional crystallographic information files can be found on the Cambridge Structural Database by requesting deposition numbers 2027043.

AUTHOR INFORMATION

Corresponding Author

*Tori Z. Forbes: tori-forbes@uiowa.edu_

Author Contributions

TZF and SEM provided resources, support and funding to carry-out the study. MS and JAS did the synthesis experiment. MS did all the chemical characterization, crystallography and experimental data analysis. JLB conducted all of the DFT calculations. MS and JLB prepared the initial draft of manuscript. All authors contributed to the writing and editing of final manuscript for the submission.

Notes

The authors declare no competing financial interests.

ACKNOWLEDGMENT

SEM acknowledges computational resources provided by the University of Iowa. This work used the Extreme Science and Engineering Discovery Environment (XSEDE),[39] which is supported by the National Science Foundation grant number ACI-1548562 though allocation TG-GEO160006. We acknowledge Prof. Aliasger Salem and Dr. Lr Jaidev Chakka (UI college of Pharmacy) for their help regarding DLS experiment. TZF and MS also acknowledge American Crystallographic Association (ACA) summer school 2019 at Northwestern University for their travel support to teach MS advanced-level crystallography. JLB acknowledges support from the University of Iowa's Dissertation Writing Fellowship.

REFERENCES

1. Keggin, J. F., Structure of the Molecule of 12-Phosphotungstic Acid. *Nature* **1933,** *131* (3321), 908-909.

2. Li, D.; Ma, P.; Niu, J.; Wang, J., Recent advances in transition-metal-containing Keggin-type polyoxometalate-based coordination polymers. *Coordination Chemistry Reviews* **2019,** *392*, 49-80.

3. Parker, W. O. N.; Millini, R.; Kiricsi, I., Metal Substitution in Keggin-Type Tridecameric Aluminum−Oxo−Hydroxy Clusters. *Inorganic Chemistry* **1997,** *36* (4), 571-575.

4. Lee, A. P.; Phillips, B. L.; Olmstead, M. M.; Casey, W. H., Synthesis and Characterization of the GeO4Al12(OH)24(OH2)128+ Polyoxocation. *Inorganic Chemistry* **2001,** *40* (17), 4485-4487.

5. Shohel, M.; Bjorklund, J. L.; Ovrom, E. A.; Mason, S. E.; Forbes, T. Z., Ga3+ Incorporation into Al13 Keggin Polyoxometalates and the Formation of δ-(GaAl12)7+ and (Ga2.5Al28.5)19+ Polycations. *Inorganic Chemistry* **2020,** *59* (15), 10461-10472.

6. Wang, W.; Fullmer, L. B.; Bandeira, N. A. G.; Goberna-Ferrón, S.; Zakharov, L. N.; Bo, C.; Keszler, D. A.; Nyman, M., Crystallizing Elusive Chromium Polycations. *Chem* **2016,** *1* (6), 887-901.

7. Muñoz, M.; Romanelli, G.; Botto, I. L.; Cabello, C. I.; Lamonier, C.; Capron, M.; Baranek, P.; Blanchard, P.; Payen, E., Al13–[X–Mo/WOn] (X=Al, Co, V, P) composites as catalysts in clean oxidation of aromatic sulfides. *Applied Catalysis B: Environmental* **2010,** *100* (1), 254-263.

8. Benito, I.; del Riego, A.; Martínez, M.; Blanco, C.; Pesquera, C.; González, F., Toluene methylation on Al13- and GaAl12-pillared clay catalysts. *Applied Catalysis A: General* **1999,** *180* (1), 175-182.

9. Stewart, T. A.; Trudell, D. E.; Alam, T. M.; Ohlin, C. A.; Lawler, C.; Casey, W. H.; Jett, S.; Nyman, M., Enhanced Water Purification: A Single Atom Makes a Difference. *Environmental Science & Technology* **2009,** *43* (14), 5416-5422.

10. Bijelic, A.; Aureliano, M.; Rompel, A., Polyoxometalates as Potential Next-Generation Metallodrugs in the Combat Against Cancer. *Angewandte Chemie International Edition* **2019,** *58* (10), 2980-2999.

11. Yeo, H. J.; Paik, Y.; Paek, S.-M.; Honma, I., Keggin-type aluminum polyoxocation/graphene oxide hybrid as a new nanostructured electrode for a lithium ion battery. *Journal of Physics and Chemistry of Solids* **2012,** *73* (12), 1417-1419.

12. Priyadarshini, M.; Shanmugan, S.; Kirubakaran, K. P.; Thomas, A.; Prakash, M.; Senthil, C.; Lee, C. W.; Vediappan, K., High energy storage of Li-ions on keggin-type polyoxometalate as electrodes for rechargeable lithium batteries. *Journal of Physics and Chemistry of Solids* **2020,** *142*, 109468.

13. Wang, G.; Zhou, J.; Li, J., Layer-by-layer self-assembly aluminum Keggin ions/Prussian blue nanoparticles ultrathin films towards multifunctional sensing applications. *Biosensors and Bioelectronics* **2007,** *22* (12), 2921-2925.

14. Chen, X.; Huang, P.; Zhu, X.; Zhuang, S.; Zhu, H.; Fu, J.; Nissimagoudar, A. S.; Li, W.; Zhang, X.; Zhou, L.; Wang, Y.; Lv, Z.; Zhou, Y.; Han, S.-T., Keggin-type polyoxometalate cluster as an active component for redox-based nonvolatile memory. *Nanoscale Horizons* **2019,** *4* (3), 697-704.

15. Furrer, G.; Phillips, B. L.; Ulrich, K.-U.; Pöthig, R.; Casey, W. H., The Origin of Aluminum Flocs in Polluted Streams. *Science* **2002,** *297* (5590), 2245.

16. Sadeghi, O.; Zakharov, L. N.; Nyman, M., Aqueous formation and manipulation of the iron-oxo Keggin ion. *Science* **2015,** *347* (6228), 1359.

17. Nyman, M., Polyoxometalates and Other Metal-Oxo Clusters in Nature. In *Encyclopedia of Geochemistry: A Comprehensive Reference Source on the Chemistry of the Earth*, White, W. M., Ed. Springer International Publishing: Cham, 2016; pp 1-5.

18. Long, D.-L.; Burkholder, E.; Cronin, L., Polyoxometalate clusters, nanostructures and materials: From self assembly to designer materials and devices. *Chemical Society Reviews* **2007,** *36* (1), 105-121.

19. Abeysinghe, S.; Unruh, D. K.; Forbes, T. Z., Crystallization of Keggin-Type Polyaluminum Species by Supramolecular Interactions with Disulfonate Anions. *Crystal Growth & Design* **2012,** *12* (4), 2044-2051.

20. Sun, Z.; Wang, H.; Tong, H.; Sun, S., A Giant Polyaluminum Species S−Al32 and Two Aluminum Polyoxocations Involving Coordination by Sulfate Ions S−Al32 and S−K−Al13. *Inorganic Chemistry* **2011,** *50* (2), 559-564.

21. Mothé-Esteves, P.; Pereira, M. M.; Arichi, J.; Louis, B., How Keggin-Type Polyoxometalates Self-Organize into Crystals. *Crystal Growth & Design* **2010,** *10* (1), 371-378.

22. Matsunaga, S.; Inoue, Y.; Mihara, K.; Nomiya, K., Synthesis and crystal structure of hexacerium(IV) cluster-containing Keggin polyoxometalate trimer. *Inorganic Chemistry Communications* **2017,** *80*, 61-64.

23. Al-Kadamany, G. A.; Hussain, F.; Mal, S. S.; Dickman, M. H.; Leclerc-Laronze, N.; Marrot, J.; Cadot, E.; Kortz, U., Cyclic Ti9 Keggin Trimers with Tetrahedral (PO4) or Octahedral (TiO6) Capping Groups. *Inorganic Chemistry* **2008,** *47* (19), 8574-8576.

24. Sakai, Y.; Yoza, K.; Kato, C. N.; Nomiya, K., Tetrameric, Trititanium(IV)-Substituted Polyoxotungstates with an α-Dawson Substructure as Soluble Metal-Oxide Analogues: Molecular Structure of the Giant “Tetrapod” [(α-1,2,3-P2W15Ti3O62)4{μ3-Ti(OH)3}4Cl]45−. *Chemistry – A European Journal* **2003,** *9* (17), 4077-4083.

25. Sakai, Y.; Ohta, S.; Shintoyo, Y.; Yoshida, S.; Taguchi, Y.; Matsuki, Y.; Matsunaga, S.; Nomiya, K., Encapsulation of Anion/Cation in the Central Cavity of Tetrameric Polyoxometalate, Composed of Four Trititanium(IV)-Substituted α-Dawson Subunits, Initiated by Protonation/Deprotonation of the Bridging Oxygen Atoms on the Intramolecular Surface. *Inorganic Chemistry* **2011,** *50* (14), 6575-6583.

26. Zhang, Z.; Wang, Y.-L.; Yang, G.-Y., An unprecedented Zr-containing polyoxometalate tetramer with mixed trilacunary/dilacunary Keggin-type polyoxotungstate units. *Acta Crystallographica Section C Structural Chemistry* **2018,** *74* (11), 1284-1288.

27. Zhao, J.-W.; Zhang, J.; Zheng, S.-T.; Yang, G.-Y., Combination of Lacunary Polyoxometalates and High-Nuclear Transition-Metal Clusters under Hydrothermal Conditions. 5. A Novel Tetrameric Cluster of [{FeIIFeIII12(μ3-OH)12(μ4-PO4)4}(B-α-PW9O34)4]22. *Inorganic Chemistry* **2007,** *46* (26), 10944-10946.

28. Wang, K.-Y.; Bassil, B. S.; Lin, Z.-G.; Haider, A.; Cao, J.; Stephan, H.; Viehweger, K.; Kortz, U., Ti7-

containing, tetrahedral 36-tungsto-4-arsenate(iii) [Ti6(TiO6)(AsW9O33)4]20−. *Dalton Transactions* **2014,** *43* (43), 16143-16146.

29. Pradeep, C. P.; Long, D.-L.; Kögerler, P.; Cronin, L., Controlled assembly and solution observation of a 2.6 nm polyoxometalate 'super' tetrahedron cluster: [KFe12(OH)18(α-1,2,3-P2W15O56)4]29−. *Chemical Communications* **2007,** (41), 4254-4256.

30. Yoshitaka, S.; Shoko, Y.; Takeshi, H.; Hideyuki, M.; Kenji, N., Tetrameric, Tri-Titanium(IV)-Substituted Polyoxometalates with an α-Dawson Substructure as Soluble Metal Oxide Analogues. Synthesis and Molecular Structure of Three Giant "Tetrapods" Encapsulating Different Anions (Br−, I−, and NO3−). *Bulletin of the Chemical Society of Japan* **2007,** *80* (10), 1965-1974.

31. Bjorklund, J. L.; Bennett, J. W.; Forbes, T. Z.; Mason, S. E., Modeling of MAl12 Keggin Heteroatom Reactivity by Anion Adsorption. *Crystal Growth & Design* **2019,** *19* (5), 2820-2829.

32. Lee, A. P.; Furrer, G.; Casey, W. H., On the Acid–Base Chemistry of the Keggin Polymers: GaAl12 and GeAl12. *Journal of Colloid and Interface Science* **2002,** *250* (1), 269-270.

33. Lee, A. P.; Phillips, B. L.; Casey, W. H., The kinetics of oxygen exchange between the GeO4Al12(OH)24(OH2)128+(aq) molecule and aqueous solutions. *Geochimica et Cosmochimica Acta* **2002,** *66* (4), 577-587.

34. Sakai, Y.; Yoza, K.; Kato, C. N.; Nomiya, K., A first example of polyoxotungstate-based giant molecule. Synthesis and molecular structure of a tetrapod-shaped Ti–O–Ti bridged anhydride form of Dawson tri-titanium(iv)-substituted polyoxotungstate. *Dalton Transactions* **2003,** (18), 3581-3586.

35. Al-Kadamany, G. Synthesis, Structure and Catalytic Activity of Titanium, Zirconium and Hafnium-Containing Polyoxometalates. Jacobs University, IRC-Library, Information Resource Center der Jacobs University Bremen, 2010.

36. Kim, G.-S.; Zeng, H.; VanDerveer, D.; Hill, C. L., A Supramolecular Tetra-Keggin Polyoxometalate [Nb4O6(α-Nb3SiW9O40)4]20− *Angewandte Chemie International Edition* **1999,** *38* (21), 3205-3207.

37. Hussain, F.; Bassil, B. S.; Bi, L.-H.; Reicke, M.; Kortz, U., Structural Control on the Nanomolecular Scale: Self-Assembly of the Polyoxotungstate Wheel [{β-Ti2SiW10O39}4]24−. *Angewandte Chemie International Edition* **2004,** *43* (26), 3485-3488.

38. Bennett, J. W.; Bjorklund, J. L.; Forbes, T. Z.; Mason, S. E., Systematic Study of Aluminum Nanoclusters and Anion Adsorbates. *Inorganic Chemistry* **2017,** *56* (21), 13014-13028.

39. John Towns, T. C., Maytal Dahan, Ian Foster, Kelly Gaither, Andrew Grimshaw, Victor Hazlewood, Scott Lathrop, Dave Lifka, Gregory D. Peterson, Ralph Roskies, J. Ray Scott, Nancy Wilkins-Diehr, XSEDE: Accelerating Scientific Discovery. *Computing in Science & Engineering* **2014,** *16* (5), 62-74.

For Table of Contents Only

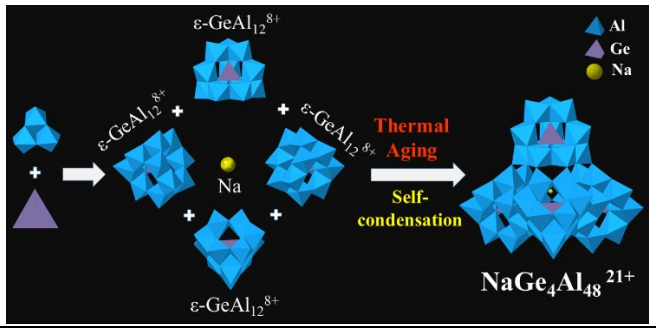

The proposed mechanism for the formation of tetrameric $Na[Ge_4O_{16}Al_{48}(OH)_{108}(H_2O)_{24}]^{20+}$ ($NaGe_4Al_{48}^{21+}$) resulting from self-condensation of ε-$GeAl_{12}^{8+}$ upon thermal aging.